11-26-2018 5:26 PM

Diagnostic Ultrasound in the Measurement of Cortical Bone Thickness in Porcine Mandibular Specimens

Diego Diaz Guerrero, *The University of Western Ontario*

Supervisor: Tassi, A., *The University of Western Ontario*

A thesis submitted in partial fulfillment of the requirements for the Master of Clinical Dentistry degree in Orthodontics

Abstract

Introduction: Ultrasound (US) is a safe, non-invasive diagnostic method that has been used in various capacities in medicine and dentistry. Periodontal bone loss, bony dehiscence, and gingival recession have been reported as potential risks of orthodontic treatment in patients who have decreased buccal/labial bone thickness. US has the potential to aid in the diagnosis of patients at risk for these possible complications of orthodontic treatment.

Purpose: To validate the use of a novel US device in the measurement of buccal cortical bone (BCB) thickness over roots in porcine mandibles.

Materials and Methods: Jaw and cortical bone models were constructed and used for software and protocol refinement. Three porcine hemi-mandibles were scanned with Micro-CT (μ-CT). BCB thickness was measured with imaging software at 12 locations per specimen (n=36). BCB thickness at these locations was then assessed using a 19MHz pulse-echo US transducer. Bone thickness was determined by assessing US wave time of flight using a calibrated speed of sound (SOS) through porcine cortical bone. Statistical analysis was done with paired t-test, Pearson correlation, and Bland-Altman plots.

Results: SOS was calibrated to 3235m/s. Mean bone thickness (+/- SD) from μ-CT was 2.06 +/- 0.76mm and 1.61 +/- 0.46mm from US. μ-CT and US thickness measurements were significantly different.

Conclusion: A handheld US device showed promise in measuring BCB thickness, but some variability exists especially when measuring thicker bone. Further improvements in the device and the algorithms used are warranted to increase the accuracy and reliability of measuring cortical bone thickness overlying roots of teeth.

Keywords

Diagnostic Ultrasound, Intra-oral Ultrasound, Cortical Bone Thickness, Periodontal Assessment, Orthodontic Complications

Acknowledgments

I would like to start by expressing my gratitude to Dr. Antonios Mamandras for giving me the opportunity to pursue my dreams of becoming an orthodontist. Thank you for welcoming me into the Western Graduate Orthodontics family and for establishing such an incredible residency program.

My most sincere gratitude also goes to Dr. Ali Tassi, my thesis supervisor. Thank you for your tireless support and guidance not only throughout the course of this project, but also my entire orthodontic education. Your passion for orthodontics and your dedication to teaching is truly awe-inspiring. Dr. Mark Pus, Dr. Khadry Galil, and Dr. Fernando Inocencio, my esteemed research committee, thank you for your valuable insight, suggestions, and thought-provoking discussion.

This project would not have been possible without the incredible efforts and assistance of Bartosz Slak and the rest of our collaborators at the Institute for Diagnostic Imaging Research as well as Joseph Umoh at Robarts Research Institute.

To my wife Marissa, thank you for your boundless support and patience during my many years of schooling. You're an incredible woman and I am honoured to share this life with you. I smile when I think about the future with you and our beautiful daughter Arianna.

To my most amazing parents, words cannot express how much gratitude I feel for everything you've done for me. Your unconditional love and support have made me the man that I am. Everything that I have accomplished is due to the morals and work ethic you instilled in me… gracias desde el fondo de mi corazón.

Table of Contents

List of Tables

List of Figures

List of Abbreviations

BCB – Buccal cortical bone

CBCT – Cone beam computed tomography

CI – Confidence interval

CT – Computed tomography

DXA – Dual-energy X-ray absorptiometry

IANC – Inferior alveolar nerve canal

IMPA – Incisor to mandibular plane angle

μ-CT – Micro computed tomography

PDL – Periodontal ligament

SOS – Speed of sound

TADs – Temporary anchorage devices

TOF – Time of flight

US – Ultrasound

UTV – Ultrasound transmission velocity

List of Appendices

Chapter 1: Review of the Literature

1.1 Ultrasound as a Diagnostic Tool

Audible sound waves are detected by the human ear within the range of 20Hz – 20 KHz.[1] Anything beyond the upper limit is referred to as ultrasound (US). The idea for diagnostic US was born out of a radar technique developed for World War II when an internal medicine resident at Lund University, Inge Edler, was driven to improve the pre-surgical diagnostics for cardiac surgery.[2] Edler elicited the help of physicist Hellmuth Hertz in the early 1950s. Hertz gained access to ultrasound equipment at a shipbuilding yard being used to test for imperfections in welded seams.[2] They both placed the device on their own hearts and realized that they could see echoes from within. The device needed to be modified and supplied with a film camera to be able to record images of the area being investigated. After modifications were made to the equipment with the help of the Siemens Company, on October 29, 1953, the first moving images of the human heart were captured.[2] This technique has since been developed into modern echocardiography.

Lund University was also where US was first used in obstetrics and gynecology. Before its widespread use in the investigation of potentially vulnerable tissues like developing fetuses and ovaries, it needed to be deemed safe. *In-vitro* experiments on pregnant and non-pregnant rats were conducted. Normal ovarian function and fertility were found in the rats exposed to US.[2] There was also no increase in intrauterine death, pre-term birth, neo-natal mortality or deformities for the exposed rats or for the second generation after exposure. Having been satisfied with its safety, Bertil Sunden and the rest of the Department of Obstetrics and Gynecology, began using US to assess fetal development in humans. US gained popularity in this field and it is now a routinely used diagnostic method for the monitoring of pregnancies worldwide. Besides its use in cardiology and

obstetrics/gynecology, US is routinely used in other fields like trauma, ophthalmology, and otorhinolaryngology.[2]

1.1.1 Principles of US

Sound can be thought of as travelling variations in pressure through a medium.[1] As for audible sound, the medium is usually air, but sound can travel through different mediums like metal, water, and human tissues. Sound travels through different tissues at different speeds depending on acoustic properties of the material like density and particle vibration. The less compressible a material is, the higher the speed of sound (SOS) is through that material. When a sound wave passes from one material to another, the wave can be transmitted (continuing to propagate), it can be reflected back to the source, or a combination of transmission and reflection can happen. Acoustic impedance is the material property that determines what will happen to the incident wave. It is determined by density multiplied by SOS in that material. If the impedance of two materials are the same or very close to one another, the incident wave will continue propagating and none to very little reflection in the form of an echo will be produced. If the impedance varies, a greater proportion of the incident wave will be reflected as an echo. If the impedance are greatly different, as in air and tissue, there is no transmission, only an echo. This is the reason behind the need for a coupling medium like US gel. The echoes that are produced when sound travels through different materials makes diagnostic US possible. Knowing the speed of sound in a material and the time between echoes produced as the wave enters and exits the material, a.k.a. time of flight (TOF), will allow you to measure the thickness of the material.

As a wave propagates through a material it weakens or attenuates. Although traveling through different materials gives off echoes that weaken the incident wave, most attenuation is due to the conversion of the sound to heat, or absorption. The degree to which a wave propagates is also influenced by scattering and the incidence angle. Scattering is the redirection of a sound wave into many directions due to a rough surface or tissue boundary. This occurs regardless of the

incidence angle, or the angle at which the incident wave approaches the tissue boundary. An incident wave that is perpendicular to the tissue boundary will result in transmission of the wave and an echo that travels back to the transducer (Fig. 1). An incident wave that is oblique to the tissue boundary will result in the transmission and reflection of the wave at an angle that is equal to the incidence angle (Fig. 2). If the two materials have impedance that are different, the

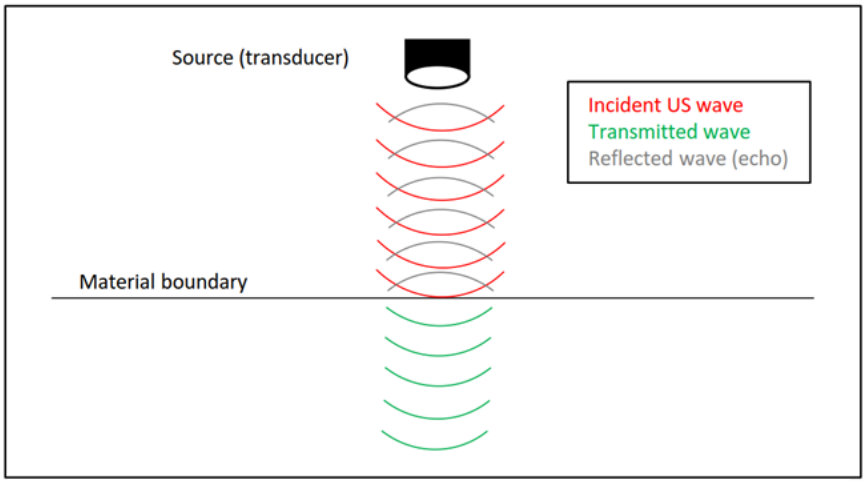

Figure 1. Incident US wave perpendicular to the material boundary. Resultant echo and transmitted wave propagating through new material.

transmitted wave is refracted and propagates at an angle that is different than the incidence angle (Fig. 3). Oblique incidence of a sound wave makes the detection of echoes by the transducer much more difficult because of reflection and refraction.

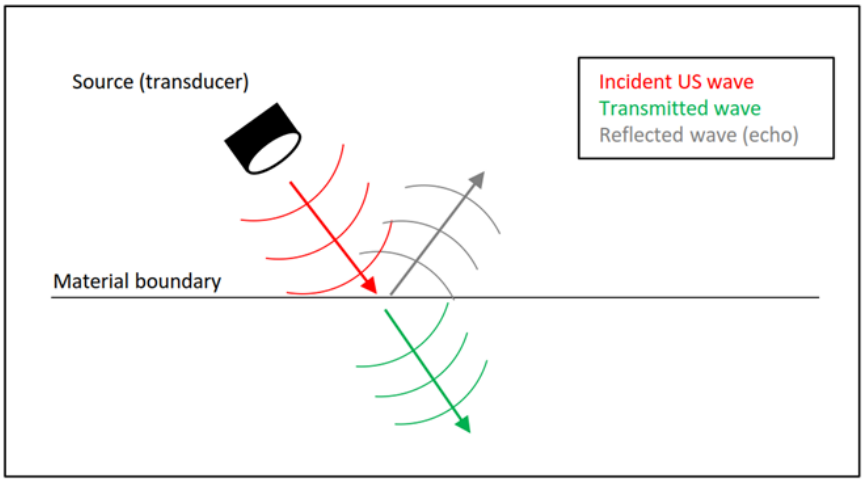

Figure 2. Incident US wave oblique to the material boundary. Reflection angle and transmission angle are the same as the incident angle if impedance between the two materials is similar.

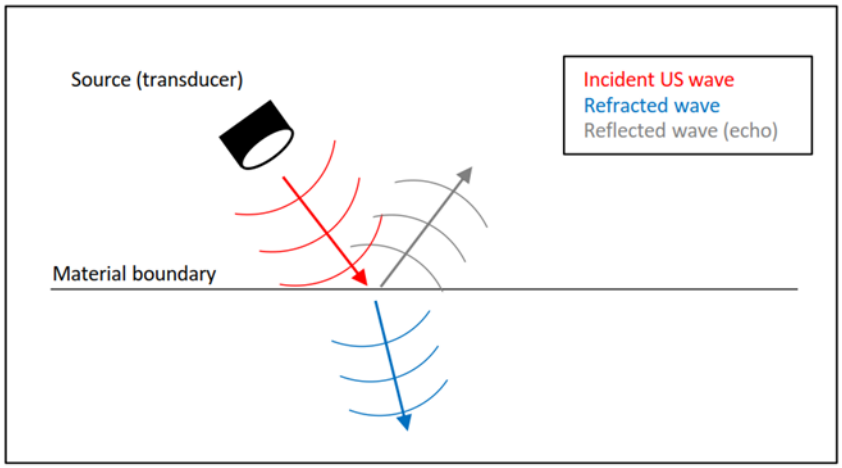

Figure 3. Incident US wave oblique to material boundary. High difference of impedance between materials results in incident and transmission angles being different resulting in wave refraction.

US devices are composed of transducers, pulsers, and receivers connected to computers and monitors that produce images interpreted by technicians or health-care professionals. Pulsers generate electrical impulses that are converted to US waves by transducers. These same transducers convert echoes that are given off by tissues into electrical impulses that go through a receiver to get converted into digital imagery in the form of A-scans, B-scans, and C-scans (Fig. 4)[3].

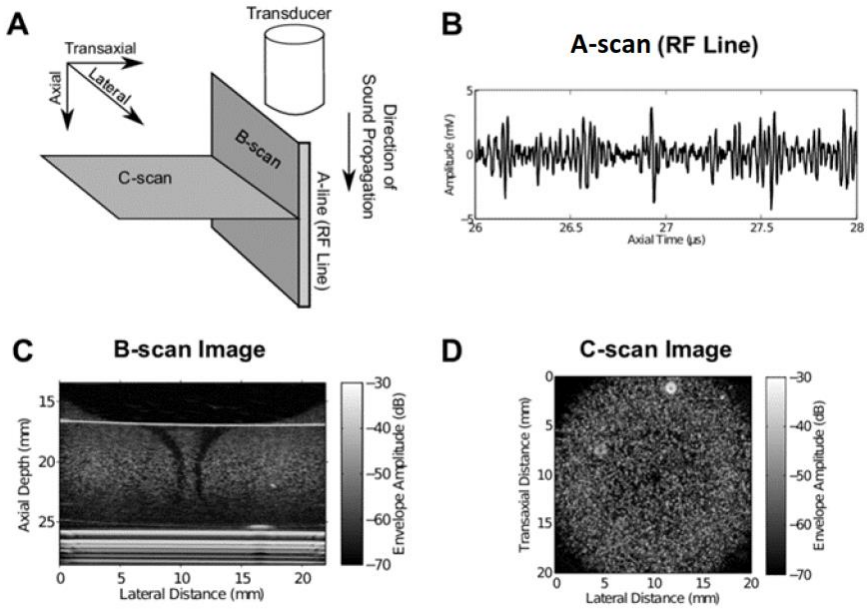

Figure 4. Ultrasound imaging. **(A)** Diagram of the orientation of the image in relation to the direction of sound propagation. **(B)** Sample A-scan showing strength of reflected echoes. **(C)** Sample B-scan showing echo causing objects/interfaces in cross-section. **(D)** Sample C-scan showing echo causing objects perpendicular to the direction of wave propagation. Reprinted by permission from Springer Nature Customer Service Centre GmbH: Springer Nature Annals of Biomedical Engineering, Quantitave Ultrasound for Nondestructive Characterization of Engineered Tissues and Biomaterials, Dalecki *et al.* 2015.

A-scans, or amplitude scans, are graphical representations of the strength of echoes detected with amplitude on the y-axis and time on the x-axis. B-scans, or brightness scans, are cross-sectional representations of tissues being investigated by US with echo causing objects and boundaries causing distinct changes in the brightness of the pixels in the image. The lighter the pixel, the stronger the echo detected. This is the most common US imagery seen in obstetrics and gynecology to investigate the developing fetus. C-scans are the least common form of imagery seen in medical US. They are derived from mechanical US where a given area is scanned with a fixed transducer that records data in the form of pixels and brightness, like a b-scan. Unlike a b-scan, the c-scan provides a two-dimensional image that maps out where the echoes were produced in that area depending on the coordinates of the transducer.

Two main types of transducers are single (focused and non-focused), and linear array which is essentially multiple transducers arranged side by side. US devices usually operate as either pulse-echo, where the same transducer emits and detects echoes, or through transmission, where one transducer emits while another transducer detects.

1.2 Diagnostic Ultrasound of Hard Tissues

By far, US in medicine has been used primarily for the diagnosis and investigation of soft tissues. However, several studies have investigated its potential use in hard tissues with promising results. Some of the more interesting and potentially beneficial hard tissue applications of US include intraoperative measurement of cranial bone thickness, US assisted pedicle screw placement in spinal fusion surgery, and the diagnosis of osteoporosis.

1.2.1 US in the Assessment of Cranial Bone Thickness

Calvarial bone has become popular amongst surgeons as a bone graft donor site in various procedures involved in reconstruction and rehabilitation of the craniomaxillofacial region.[4] Knowing the dimensions of the area of interest at the donor site is critical especially when dealing with cranial bone. Inadvertent penetration of the cranial cavity can cause cerebrospinal fluid leaks, mechanical brain injuries and intracranial hematomas.[4] Although computed tomography (CT) scans are used in these surgeries, difficulty in extrapolating information from the scans to real time surgical situations has been reported.[5]

Elahi *et al.* [4,5] demonstrated the potential effectiveness of using US devices to measure cranial bone thickness in two separate studies. The first was done on human cadaveric skull specimens with a spherically focused 6.2MHz pulse-echo transducer while the second study was conducted on live porcine skulls with a 1MHz non-focused pulse-echo transducer. In both studies, TOF of the incident US wave and its corresponding echoes from A-scans were used to determine cranial bone thickness in specified locations. These were compared to gold standard digital caliper measurements. The conclusion from both studies was that skull thickness measurements obtained with US were reliable and accurate enough to be useful in preoperative and intraoperative situations for bone harvesting procedures.[4,5]

Tretbar *et al.*[6] also investigated the use of US in cranial bone thickness. They used 3 different US techniques, one of them involving the novel SonoPointer™ US device with a 2.25MHz transducer to investigate thickness of human cadaver skulls. They also compared US measurements to those obtained by digital calipers and found good agreement between the methods. Although they acknowledge further testing is needed, they suggest that the SonoPointer™ shows promise to be used as a stand-alone device in cranial surgery.[6]

1.2.2 US in Spinal Surgical Procedures

Spinal surgery is a very delicate and complex procedure with potentially dire risks. Spinal fusion is a common procedure done to immobilize segments of the vertebral column with rigid fixation as treatment for fractures, curvature deformities, excessive back pain, and degenerative diseases.[7] The surgery involves prepping of a pilot hole with blunt tipped cannulation which relies on tactile feedback by the operator. This feedback often results in multiple path corrections which increases the displacement of cancellous and possibly cortical bone resulting in increased surgical trauma and decreased post-surgical stability. The proximity to vital neurovascular structures and the limited intraoperative visibility increases the risk of devastating post-surgical consequences. Due to these irreversible and life-altering risks, research into improving the safety of spinal surgery is warranted.

Various methods of US have been investigated in vitro with respect to assisting in spinal surgery including using pulse-echo and through transmission transducers ranging from 1-10MHz with A-scan and B-scan imagery.[7–9] Like the research conducted for cranial surgery applications, A-scan imagery with pulse-echo transducers appears to be the most clinically practical and promising.

1.2.3 US in the Diagnosis of Osteoporosis

Osteoporosis is a disease most commonly found in elderly women that results in reduced bone mass, volume and density increasing the likelihood of fractures. It often goes underdiagnosed and undertreated by primary care physicians.[10] The diagnosis of the disease is done by measuring bone mineral density in the hip and spine by dual-energy X-ray absorptiometry (DXA).[11] Because of the bulky instrumentation, radiation, and cost, DXA is not a practical screening tool for primary care physicians.[12]

Decreased cortical bone thickness of the radius as measured with peripheral quantitative CT scans has been associated with fractures in patients undergoing hemodialysis.[13] Karjalainen *et al.* [11,12,14,15] have endeavored to use US to

measure cortical bone thickness in the distal radius, distal and proximal tibia and femur in order to estimate bone mineral density and potentially screen for osteoporosis and risk of related fractures. In an earlier study, they showed that cortical thickness measurement with a focused 2.25MHz US transducer correlated well with measurements obtained by CT scans both *in-vitro* and *in-vivo*.[11] Subsequent studies demonstrated that US measurements with a focused 3.0MHz transducer had the potential to be a safe, practical, and effective first-line screening tool for osteoporosis in at risk populations by estimating bone mineral density.[12,14,15]

1.3 Diagnostic Ultrasound in Dentistry

US has been investigated in the context of dentistry with the primary areas of focus being periodontology and implantology. The draw of being able to image and assess periodontal structures in a non-invasive, non-radiative manner has driven research in the area. As for implantology, US has been investigated as a possible means to conveniently and effectively assess both the quality of bone in prospective dental implant sites as well as identify vital structures to be avoided during implant surgery. Of the few studies regarding orthodontics, most have dealt with therapeutic US, an exciting potential adjunct therapy but beyond the scope of this dissertation. The few studies that have looked at diagnostic US have attempted to use it to identify proper locations for placement of temporary anchorage devices (TADs) by measuring soft tissue thickness.

1.3.1 US in Periodontology

US had been commonly used in the field of medicine for decades before research into its potential applications for dentistry began in the mid-1980s. Some of the earliest investigations into US in dentistry were conducted in the field of periodontics. A German group out of the University of Stuttgart led by Lost and Nussle investigated the use of US in the imaging of periodontal structures.[16] They

made 12 parallel-cut bone samples ranging in thickness from 0.1-2.0mm and were interested in finding out which prepared thicknesses of bone were penetrated by different frequency US pulses. They also investigated what width of space, representing the periodontal ligament (PDL), is distinguished by US scanning with the three transducers used (5MHz, 10MHz, 20MHz). Their experiments were conducted in a water bath with fixed transducers and a digital US measuring and analysis system that generated A-scans analyzed for echo peaks. All three transducers were able to detect a minimum mock PDL width of 0.16mm and penetrate bone 1.5mm thick but only the 5MHz transducer was shown to penetrate the bone 2.0mm thick.[16] They conducted further studies with the 10MHz and 20MHz transducers on porcine periodontium in an attempt to detect the height of the alveolar crest with both A-scans and B-scans.[17,18] They were successful in identifying the PDL space with both frequency transducers but the identification of the location of the alveolar crest was more accurately determined by the 20MHz US probe.[18] In both studies, they compared their measurements and US findings by histological assessment. Because of the relatively small sample size, they did not do any statistical analysis but concluded that with further technological innovation and research, pulse echo US is a promising non-invasive method for determining the height of the alveolar crest in humans.[18]

Tsiolis *et al.*[19] also attempted to use US in periodontal tissue assessment and were particularly interested in dimensional assessments of these structures. They used a 20MHz US device that was designed to have the transducer move across the intended target over a 15mm by 6.25mm section with the gathering of US data taking less than a second. They used porcine jaw specimens and measured the distance between a prepared notch on a tooth to the alveolar crest. Measurements from US, gingival probing, and from direct histological assessment were compared. Their results showed that measurements derived from US and direct histological assessment had the narrowest limits of agreement and US was the most repeatable.[19]

Research has also been done on the effectiveness of US measurement of gingival thickness to establish a non-invasive, quantitative method of diagnosing gingival biotypes. Eger *et al.*[20] used a 5MHz pulse-echo US device on porcine gingiva to measure gingival thickness and compare it to the gold standard of measurement with an endodontic file and rubber stopper. Both types of measurements were highly correlated (r^2=0.906) and the US measurements showed a high degree of reproducibility and consistency.[20] Comparable results indicating a high level of accuracy of US gingival thickness measurements were found in various other studies using 25MHz, 40MHz, and 50MHz transducers.[21–23]

The imaging of hard tissues with US is far more technically difficult than that of soft tissues. Advances in US technology and software have made the US assessment of periodontal hard tissues a possibility; recent studies have investigated this potential. A 20MHz pulse echo transducer was used by Radu *et al.*[24] to assess the lingual periodontium of 20 teeth in four porcine mandibles. They assessed B-scan images obtained by the US device and measured the PDL space, thickness of attached gingiva, and thickness of lingual cortical bone. The authors stated that their findings were statistically similar to the measurements of pig periodontium in veterinary literature but did not elaborate on statistical methods used.[24]

Because of the margin of error associated with periodontal probing as well as the lack of information obtained from radiographs regarding the buccal/lingual aspects of alveolar bone, Nguyen *et al.*[25] also studied the use of an US device to image porcine periodontal structures. They used a multi-element phased array 20MHz US device to assess the anterior portion of a pig mandible and compared their findings with dental cone beam computed tomography (CBCT). The measurements they used were the distance from the gingival margin to the cemento-enamel junction, gingival margin to the alveolar crest, and the thickness of the alveolar crest. They reported relatively good agreement between the methods with a tendency of US to slightly underestimate the measurements relative to CBCT.

The biggest discrepancy was between the gingival margin to the alveolar crest measurements but they were still within a percentage difference of 10%.[25]

Degen *et al.*[26] analyzed the accuracy of measuring cortical bone thickness with US compared to CBCT with stereomicroscopy measurement as a reference on bovine rib models. The authors used both low frequency (5MHz) and high frequency (50MHz) transducers and B-scan imagery to determine thickness in 10 bovine ribs simulating a section of a jaw bone, with dental implants placed into them. Measurements were done directly over the implant as well as 4mm on either side of it. They found that US measurements deviated from the stereomicroscopy standard by a mean of 10.3% while CBCT deviated by a mean of 9.2%. They also reported that US measurements directly over the implant were more accurate than those from CBCT.

1.3.2 US in Implantology

For an excellent outcome, dental implants require sufficient amounts of good quality bone to ensure primary and secondary stability. In regions like the maxillary anterior, an understanding of soft tissue thickness is necessary to be able to predict how the tissues will respond to an implant and to plan for success in these esthetically sensitive areas. Furthermore, vital structures like neurovascular bundles must be avoided when placing dental implants. Research has been done to assess the use of US technology in these and other areas.

Culjat *et al*.[27] were interested in assessing the effectiveness of locating submerged dental implants in porcine models with a novel US device. They did so in the hopes that US could be useful in detecting precise implant locations in two-step implant surgeries leading to a less traumatic and invasive second step. The transducer had a range frequency of 5MHz-16.1MHz and used the pulse-echo method. The models were made of porcine ribs and designed to mimic implants submerged in a bony edentulous ridge of alveolar bone. Pig muscle was tightly layered over the implant/rib model with a final soft-tissue thickness of 5mm

mimicking gingiva. Detection of the implant was done by assessing the reflected echoes with the implants expected to reflect more sound waves than cancellous bone. The device was able to locate submerged dental implants to within 0.2mm of their center and accurately measure the amount of soft tissue over the implant and bony surfaces.[27]

The need for a non-invasive diagnostic tool to evaluate the quality of bone in possible implant placement locations has driven further studies regarding US in implantology. A commonly used bone quality classification system was described by Lekholm and Zarb in 1985.[28] It classifies cancellous bone as D4, with a feeling of drilling into Styrofoam and cortical bone as D1, with a feeling like drilling into oak wood. This is an intra-operative assessment and is dependent on tactile feedback at the time of surgery. Although dental CBCT is now used fairly routinely during implant surgeries, it may not be reliably used to assess bone quality with Houndsfield unit thresholds, especially in areas with thick cortical bone.[29] The Houndsfield scale is a method for assessing radiodensities from CT images. More dense and radiopaque materials have higher Houndsfield unit measurements.

Klein *el al.*[29] used a through transmission caliper-style US device with 2 transducers, a sender at 1.2MHz and receiver, to measure intraoral ultrasound transmission velocity (UTV) in various edentulous regions of 108 patients. Areas with typically poor alveolar bone quality like the maxillary posterior had significantly lower UTV than areas of high bone quality like the posterior mandible[29].

Kammerer *et al.*[30] investigated UTV in assessing bone quality in an *ex-vivo* study. Cortical, cancellous and mixed bone models were assessed with US, two-dimensional histomorphometry, CBCT, and micro computed tomography (μ-CT). A high correlation was found between all methods in their ability to differentiate different bone types/density and thus bone quality for implant placement. Follow up studies showed that UTV is also highly correlated with other methods of assessing primary implant stability such as radiofrequency analysis and the push-out test in cortical, cancellous, and mixed bone models.[31]

US has further been investigated as a potential intraoperative tool during implant surgeries. A group led by Machtei and Zigdon-Giladi used a novel handheld US device in vivo to attempt to measure the distance from the bottom of the implant osteotomy to various anatomical landmarks.[32] In the first of their studies, they recruited 14 patients that were to receive implants in the posterior maxilla and mandible. After pilot hole preparation, they measured the distance from the bottom of the osteotomy to the maxillary sinus and inferior alveolar nerve canal (IANC) with the US device and by direct measurement on a panoramic radiograph. They found strong correlation between the methods of measurement when considering the IANC but not for the maxillary sinus.[32]

This led to a follow up study where the authors focused only on the IANC.[33] Ten patients needing posterior mandibular implants were recruited for this study. Osteotomy depth and residual distance from the osteotomy to the IANC were made with the US device, from a panoramic radiograph, and from a combination of preoperative CBCT and direct clinical probe measurements. US measurements showed good agreement with the other methods of assessment with the highest correlation being with the gold standard of pre-operative CBCT + direct clinical measurement.[33] Unfortunately, the authors didn't elaborate on the specifics of the US device (frequency or method used) but nevertheless, their results demonstrate the potential for US to be used as an intra-operative tool during implant surgeries.

The ability of US to detect vital structures like neurovascular bundles, such as those that are to be avoided during implant surgery, has led to US research in the field of anaesthesia. Nerve blocks can be technique sensitive and US guided anaesthesia can potentially result in improved nerve block quality, shorter procedure times, and lower rates of complications like paresthesia after the procedure.[34] US was successfully used *in-vitro* to locate the greater palatine foramen in cadavers and *in-vivo* to assist in the administration of a greater palatine nerve block in patients undergoing dental procedures.[35]

Using dental implants as orthodontic anchorage was first reported by Linkow in the early-1970s.[36] This led to the idea of using temporary implants in

orthodontics and TADs are now commonly used in complex cases. Much of the research surrounding diagnostic US in orthodontics has been focused on determining soft tissue thickness prior to placing TADs to ensure better stability. The thickness of both soft tissue and cortical bone are factors in TAD stability.[37] Thin gingival tissue and thick cortical bone in areas where TADs will be placed is ideal.[37] Cha *et al.*[38] used a 5MHz US device to measure gingival thickness in areas where TAD placement is common. The authors stated that the device was previously validated, so no controls or other methods of measurement were used. They compared their gingival thickness measurements to those in previously reported literature and ultimately ended up concluding that US devices may help orthodontists decide where to place TADs to ensure better stability.[38]

1.4 Periodontal Complications of Orthodontic Treatment

Although a previous history of periodontal disease is not a contraindication for orthodontic treatment, active disease must be treated and deemed stable prior to commencement. Patients must also show an ability and desire to keep meticulous oral hygiene habits. Even with adequate oral hygiene and no previous periodontal disease, orthodontic treatment can result in periodontal complications if the alveolar housing isn't considered during diagnosis and treatment planning by the orthodontist.[39] The most common sequelae of inadvertently moving teeth out of the alveolar housing is bony fenestration, dehiscence, and gingival recession.[40] Orthodontic movements that are most often responsible for these complications are excessive expansion in the maxillary posterior segments, proclination of the upper and lower incisors, and retroclination and retraction of the lower incisors. This is particularly a concern when dealing with skeletal discrepancies that are being treated with non-surgical dental compensation.[40]

1.4.1 Periodontal Complications of Maxillary Expansion

Maxillary expansion, used in the treatment of transverse maxillary deficiency and crowding, can be achieved with a variety of devices. Successful expansion is more predictably accomplished prior to adolescence as the mid-palatal suture becomes more and more interdigitated and tortuous with age.[41] Once skeletal expansion is no longer possible, dental expansion by labial crown tipping becomes the primary mechanism of action. This has been thought to increase the likelihood of periodontal complications in at risk patients.

Greenbaum and Zachrisson retrospectively studied the effects of rapid and slow expansion with different types of appliances (Modified Haas and Quad Helix) on the periodontal structures compared to a non-expansion control group.[42] They measured levels of marginal alveolar bone, attachment levels from the CEJ, probing depths, and width of keratinized gingiva directly. Although there were minimal significant differences in the parameters studied, they did find that of the patients that had bony dehiscence, most were in the rapid expansion group.[42]

A similar, more recent prospective study was conducted using spiral CT to assess the periodontal effects of maxillary expansion with Haas and Hyrax expanders.[43] Pre and post-expansion CT scans were conducted to measure buccal and lingual bone thickness at both time points. Both types of expanders resulted in decreased buccal bone plate thickness and increased lingual bone plate thickness. The expansion also caused bone dehiscence on the anchor teeth with it being worse in the Hyrax group. The likelihood of dehiscence was higher if the patient had thin buccal cortical bone initially.[43] This finding was consistent with that of a study by Rungcharassaeng *et al*.[44] Besides finding a correlation between initially thin buccal bone and a further decrease in buccal bone thickness due to expansion, patient age and amount of expansion were also found to be factors.[44]

1.4.2 Periodontal Complications of Excessive Proclination or Retraction of Incisors

Increasing arch length for the purposes of treating crowding can also be accomplished by proclination of the upper and lower incisors. This is an intended, and often unintended, consequence of antero-posterior discrepancy correction. Artun *et al.*[45] cephalometrically identified patients that underwent a minimum of 2mm labial movement of the lower incisors and patients who had no lower incisor movement as part of their orthodontic treatment. Thirty patients in the labial movement group and 21 patients in the no movement group were available to attend a follow up examination at 7.83 years and 9.38 years respectively post-treatment. All patients selected had treatment with an activator and extra-oral traction as well as a period of fixed appliances initiated in the mixed dentition. Amount of recession, width of keratinized tissue, and probing depths were evaluated by measurements on study models, clinical photos, and clinical exams. Interproximally, distance to the alveolar bone was measured clinically by bone sounding under local anesthesia. At follow up, recession was present on 12 teeth in 8 of the 30 subjects in the labial movement group while only present on 2 teeth in 2 of the 21 no movement group.[45] Their findings however, weren't statistically significant for any of the measured outcomes. They hypothesized that the young age at the time of treatment allowed for adaptation and probable repair of bony dehiscence.

The authors conducted a similar study that focused on investigating periodontal issues in class III patients who underwent lower incisor decompensation/proclination prior to surgical treatment of their mandibular prognathism.[46] These patients, in contrast to the previously mentioned study, were all adults with an age range of 19-41 years. Two groups were selected based on amount of proclination of the lower incisors in the pre-surgical orthodontic phase. Group 1 included patients whose incisor to mandibular plane angle (IMPA) changed by greater than 10 degrees while Group 2, the control, included patients whose

IMPA changed by less than 2 degrees. The same periodontal parameters as in the previously mentioned study were assessed. Group 1 had significantly more teeth develop dehiscence and recession during both active treatment ($P<0.001$) and during the 3-year recall period ($P<0.01$).[46]

Periodontal complications can also be seen with excessive retraction of mandibular anterior teeth. Sarikaya *et al.*[47] assessed the buccal and lingual cortical plates in 19 bimaxillary protrusive patients treated with first bicuspid extractions and maximum anchorage retraction of anterior teeth. They used lateral cephalograms and CT scans taken pretreatment and 3 months post-retraction to assess bone thickness at the crestal, mid-root, and apical level. Bone levels buccal to the maxillary teeth showed no significant differences but lingual bone thickness decreased significantly both at the mid-root and crestal levels. For mandibular teeth, labial bone thickness decreased significantly at the crestal level. Lingual cortical plates decreased significantly at the crestal level, mid-root level and for some teeth, apical level. Of the 19 patients studied, 11 had at least one mandibular incisor that developed a significant lingual bony dehiscence. These periodontal issues were not evident during clinical examination or in the lateral cephalogram but were clearly present in the CT scan.[47] Their findings are supported by various animal studies showing similar detrimental effects to the periodontium when orthodontic tooth movement pushes the limits of the bony alveolar housing.[48–50]

Jager *et al.*[51] assessed periodontal bone defects in 43 patients who underwent previous orthodontic treatment using dental CBCT. Their results were consistent with previous studies and showed a significant decrease in both alveolar bone height and thickness during orthodontic treatment with it being more prevalent in patients over 30 years old. Although they acknowledge the multifactorial nature of bone loss, they recommend pre-treatment CBCT to assess periodontal bone in patients over 30 years.[51]

1.4.3 Dental CBCT in the Assessment of Bony Defects in Orthodontics

Because of the limitations and geometry of two-dimensional radiography, it is not a reliable method for detecting buccal and lingual periodontal bone loss.[52] CBCT on the other hand, does not have the same limitation of anatomical superimposition. Some studies have shown CBCT to be fairly accurate in assessing periodontal defects in three dimensions.[39,51,52] Other studies have shown that CBCT has other limiting factors like voxel size and scatter radiation that could question its reliability.[53,54]

Leung *et al.*[54] evaluated the accuracy and reliability of CBCT for measuring alveolar bone height and bony dehiscences and fenestrations. In their study on 13 dry human cadaver skulls examining 334 teeth, they concluded that CBCT with a voxel size of 0.38mm at 2 mA can be used to accurately measure alveolar bone height within 0.6mm. They also found that CBCT was more accurate at detecting bone fenestrations than dehiscence.[54]

Patcas *et al.*[55] also evaluated the accuracy of CBCT in the linear measurement of bone. They used 2 resolutions of CBCT (0.125mm and 0.4mm voxels) to conduct vertical and horizontal bone measurements of the mandibular anterior area in 8 intact cadaver heads. Thickness of buccal cortical bone was used as the horizontal measurement. CBCT measurements at both resolutions were then compared to direct anatomical measurements done after the removal of the soft tissues. Both resolutions of CBCT proved accurate and were in agreement with direct measurements as shown with Bland-Altman plots.[55] The authors also noted that there is a risk of overestimating both fenestrations and dehiscences on CBCT and that bone thickness of less than 1mm is more difficult to accurately measure, even with a high-resolution image.[55] A recent systematic review however, concluded that CBCT may be useful in assessing periodontal risk prior to initiating orthodontic therapy and can allow clinicians to conduct preventative or interceptive periodontal therapy like soft tissue or bone grafting.[56]

The use of CBCT in orthodontic diagnosis and treatment planning has become more and more popular. Indications for its use include the management of impacted canines, cleft lip and palate, and in the assessment of skeletal discrepancies requiring surgical procedures.[57] More uses are being elucidated like craniofacial morphometric analyses/superimpositions, airway evaluation, and assessing alveolar housing/boundaries prior to tooth movement.[57] Although more uses in orthodontics are being discovered, CBCT should only be indicated when conventional radiography and a thorough clinical examination would not give adequate information.[58] A drawback of routine CBCT use is its significantly higher effective dose of radiation than conventional radiography. A range of 20-599 μSv has been reported, depending on the machine and settings, compared to 9-26 μSv for a panoramic radiograph.[59]

Chapter 2: Objectives and Hypothesis

2.1 Rationale for the Investigation

Potential periodontal complications of orthodontic treatment are a concern that should be kept in mind by the orthodontist when diagnosing and treatment planning a case. Screening for the likelihood of these issues developing in a patient is primarily done by visual assessment of gingival biotype and amount of attached gingiva present.[56] Assessing the soft tissues provides only minimal, if any, information on the status of the bony periodontal structures. Several studies have shown an increased likelihood of developing periodontal complications when a thin buccal cortical plate is present initially.[39,43,44,60–62]

CBCT is a diagnostic method that can be used to evaluate underlying bone for dehiscence, fenestration, and thickness. Because of its ionizing radiation and the average age of orthodontic patients, it would not be without significant risk to suggest routine use of CBCT as part of a diagnostic workup, especially if an alternative was available. Hence, there exists a need for a non-radiative, cost-effective, and reliable method to assess cortical bone thickness prior to starting orthodontic treatment.

μ-CT is an accurate and reliable method to assess bone structure and architecture but it is not practical for use in a clinical setting due to the size of machinery and radiation exposure.[63] Because of its ease of use however, it has mostly replaced traditional histomorphometry, a destructive laboratory method, for the evaluation of bone microarchitecture in the research setting and is seen as a gold standard in the field.[63] For bone thickness measurements, μ-CT has also been shown to be as accurate as histomorphometric and direct histological analysis on bone specimens.[64,65]

2.2 Purpose of the Study

The objective of this investigation was to validate the use of a novel US device in the measurement of cortical bone thickness overlying roots of teeth in porcine mandibular specimens.

2.3 Hypothesis

Cortical bone thickness measurements in porcine mandibular specimens obtained with a novel US device will be statistically similar to measurements obtained with the gold standard μ-CT.

Chapter 3: Materials and Methods

3.1 Proof of Concept: Jaw and Cortical Bone Models

A jaw model was constructed for proof of concept validation and software algorithm development and refinement. It was made with 14 previously extracted and desiccated human teeth embedded in epoxy resin and alumina powder composite materials simulating cortical and cancellous bone (Fig. 5) (True Phantom Solutions, Windsor, CAN). The model jaw measured 2cm x 2.5cm x 14.5cm. The materials were previously designed and validated to mimic the acoustic properties of human cortical and cancellous bone.[66] The model was scanned in an acoustic microscope with different frequency focused and non-focused transducers (1MHz, 2.25MHz, 25MHz) with both through transmission and pulse echo methods.

Figure 5. Constructed jaw model with embedded teeth.

Through transmission with 2.25MHz transducers, one on either side of the model produced promising C-scan imagery (Fig. 6). The cancellous bone made it difficult to obtain reliable A-scan or B-scan imagery and accurately detect roots with either method so a smaller model with only cortical bone over root structure was

constructed for further software and algorithm testing. The model consisted of a human mandibular central incisor embedded in the epoxy resin and alumina powder composite cortical bone material. It measured 2cm x 2.5cm x 0.6- 0.8mm.

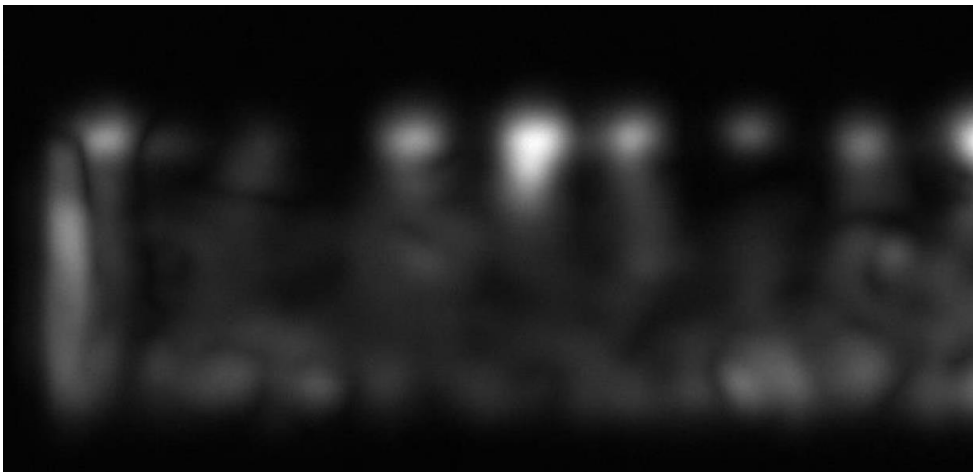

Figure 6. US C-scan image obtained from scanning with 2.25MHz transducers and through transmission method in acoustic microscope.

3.1.1 μ-CT Assessment

The cortical bone model was μ-CT scanned at 154μm sections with 120kV and 20mA with an eXplore Locus Ultra CT scan system (General Electric, Boston, USA). Images were reconstructed at 308μm resolutions. Microview imaging software (Parallax Innovations, Ilderton, CAN) was used to view and qualitatively assess cortical bone material thickness and embedded root structure form.

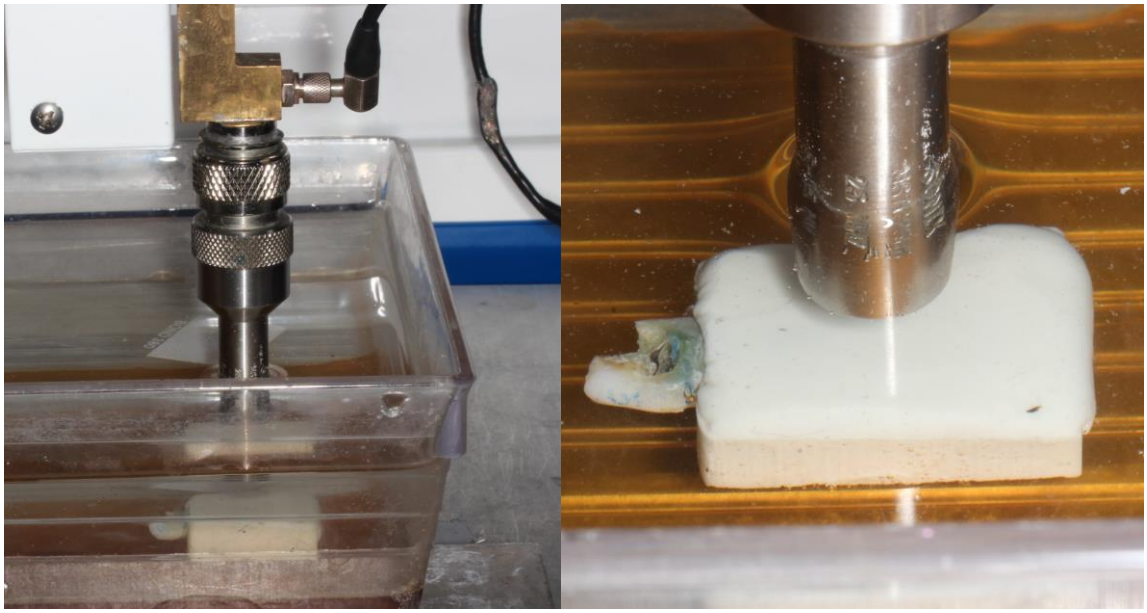

Figure 7. Bone model being US scanned in a water bath with an acoustic microscope using a 25MHz transducer.

3.1.2 US Assessment

The cortical bone model was mechanically scanned in a water bath with an ultrasonic acoustic microscope (Tessonics, Windsor, CAN) using a 25MHz single, focused transducer (Fig. 7). The scan was conducted over an area of 20mm x 20mm. Custom software developed in Matlab (Mathworks, Boston, USA) by our collaborators at the Institute for Diagnostic Imaging Research was used to gather and assess US data. A-scan, B-scan, and C-scan imagery was used to qualitatively assess cortical bone and root form. The C-scan was used to landmark over the middle of the root and draw comparisons with the x-plane from the μ-CT scan. The B-scan was used to draw comparison with the z plane from the μ-CT scan. A-scans were obtained from points over the middle of the root to assess TOF of US waves between the surface of the cortical bone and the root. TOF with a known SOS in a given material is used to give the distance travelled by the echoes with the formula:

$$distance = \frac{SOS\ x\ TOF}{2}$$

The SOS in the cortical bone model material used was previously reported as 3100m/s.[66] Trials on the cortical bone model allowed for experimenting with

algorithms and optimizing the software's ability to detect A-scan peaks associated with cortical bone and root interfaces.

3.2 Porcine Samples

Four hemi-mandibles were obtained from pigs slaughtered for human consumption. The mandibles were sectioned at the midline and were from two pigs with no indication of their age given by the abattoir. Each specimen was individually packaged, labelled and stored at 0 degrees Celsius until micro-CT scans and US scans could be completed. One specimen was used for testing and calibration of the US device while the other three were used for measurements and data collection.

3.2.1 μ-CT Measurement of Cortical Bone Thickness

Specimens were μ-CT scanned at 154μm sections with 120kV and 20mA with an eXplore Locus Ultra CT scan system (General Electric, Boston, USA). Images were reconstructed at 308μm resolutions. Microview imaging software (Parallax Innovations, Ilderton, CAN) was used to view, analyze, and measure specimens.

Locations where cortical bone thickness was to be measured were selected over the roots of the first and second premolar based on porcine dental anatomy.[67] 12 points were identified per specimen by using a maximum intensity projection image constructed from the μ-CT scan (Fig. 8). A baseline was constructed between the cusp tips of the first and third premolars. Parallel lines were made at 12mm, 14mm, and 16mm. Each of these lines had 4 points of interest, directly over the roots of the teeth. Lines perpendicular to baseline were drawn through the first and second premolar cusp tips to provide a landmark to measure distance from the points of interest and record exactly where cortical bone thickness measurement was done.

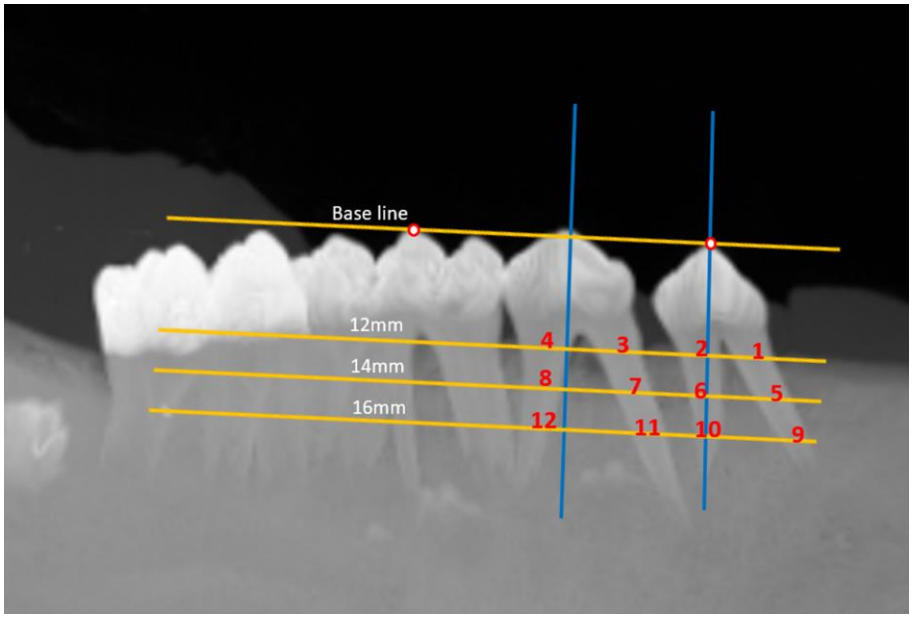

Figure 8. Points where bone thickness is to be measured identified on a μ-CT maximum intensity projection for correlation with physical samples. Baseline and 12, 14, 16mm lines (yellow), and baseline perpendicular premolar cusp tip lines (blue) identified.

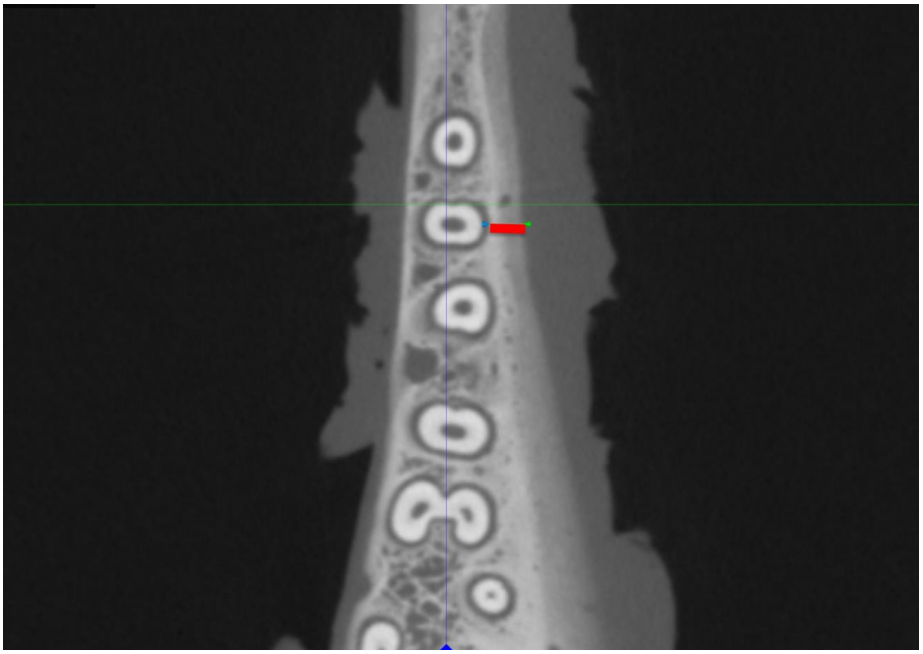

Figure 9. Section of the 12mm plane with cortical bone measurement line (red) over root corresponding to point #2.

μ-CT image planes were reoriented to make the x-plane parallel with the baseline. The y-plane and z-plane were reoriented to ensure that thickness measurements were done perpendicular to the surface of the root/PDL. Microview measuring tool was used to measure the thickness of the cortical bone at the selected points in the z-plane (Fig. 9).

An additional measurement in the x-plane was obtained from each point away from the baseline perpendicular cusp tip line to be able to transfer the point directly onto the specimen and reproduce the cortical bone thickness measurement with the US device (Fig. 10).

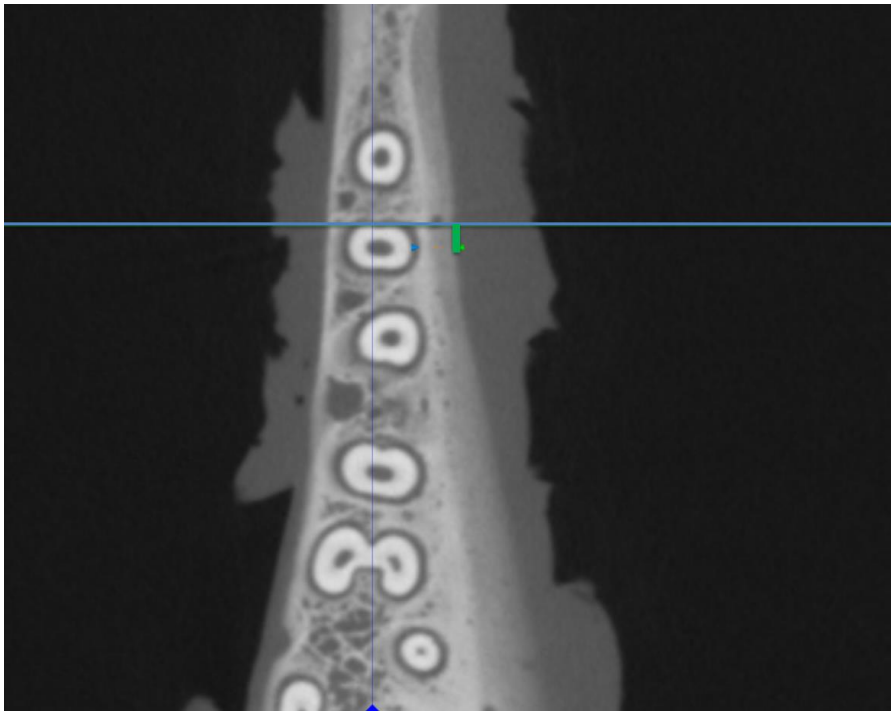

Figure 10. First premolar cusp tip line (blue) with distance measurement (green) from point where bone thickness was assessed.

Figure 11. Intra-oral US device with ruler for size comparison.

3.2.2 US Measurement of Cortical Bone Thickness

A handheld and compact US device prototype, designed for intraoral use, with a 19MHz pulse-echo transducer (Tessonics, Windsor, CAN) was used for the experiment (Fig. 11). The device had a spherically focused transducer with a probe tip diameter of 1.5mm. It was connected to a computer running custom software developed in Matlab (Mathworks, Boston, USA) by our collaborators.

The software was designed to detect three distant peaks in A-scan imagery which would theoretically correlate with tissue boundaries of probe tip and gingiva, gingiva and cortical bone, and cortical bone and PDL space/root (Fig. 12). The custom software and algorithms use the TOF between echoes and a calibrated SOS through cortical bone to give a distance reading interpreted as bone thickness.

A sample of cortical bone was removed from a specimen for SOS calibration. The sample was trimmed and polished to be square shaped, flat and 1mm thick. Digital calipers were used to measure the sample 10 times at random points for thickness giving the distance the US waves and echoes would travel. US measurements of the time of flight through the sample were conducted 10 times at random points. Mean thickness and mean time of flight were used to calculate the SOS with the formula:

$$SOS = \frac{2\ x\ distance}{time}$$

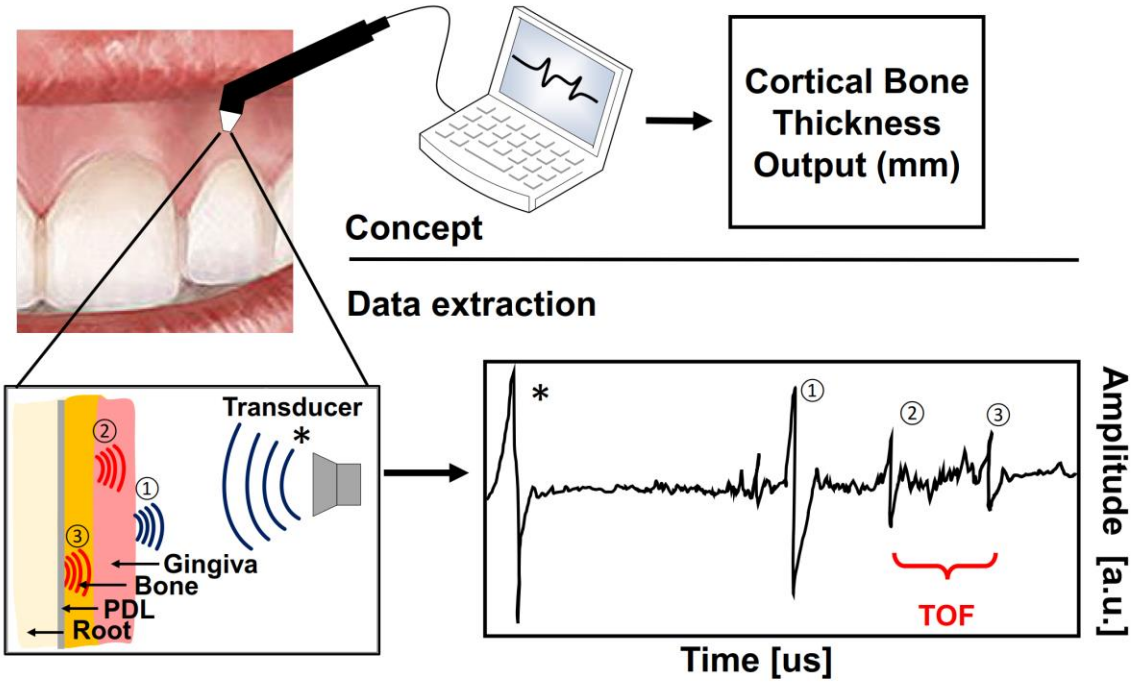

Figure 12. Concept and data extraction of measuring buccal cortical bone thickness with an US device. Pulses from the transducer are reflected as echoes from different tissue interfaces. ①= probe/gingiva interface, ②= gingiva/bone interface, ③= bone/PDL interface. Time of flight (TOF) is the time difference between echoes from gingiva/bone and bone/PDL interfaces.

Specimens were prepared by removing muscular and dermal tissue in proximity to the points of interest without damaging the overlying gingiva. The soft tissues were patted dry and 12mm, 14mm, and 16mm lines from baseline (line

connecting first and third premolar cusp tips) were drawn with an indelible surgical skin marker on the gingiva. Perpendicular lines were drawn through the first and second premolar cusp tips. The distance from these lines, where bone thickness was measured, was obtained from μ-CT imaging and the points were marked on the specimen.

The probe tip of the US device was held on the marked points during data collection with ultrasonic gel being used as a coupling medium (Fig. 13). The algorithms were constructed to collect 20 successful A-scan readings and average them to give the thickness measurement. The probe tip was held perpendicular to the surface of the specimen. Slight correction to the tip angulation was necessary at times to facilitate successful A-scan reading. Data was first collected from the 12mm line (points 1-4), then 14mm line (points 5-8), and lastly the 16mm line (points 9-12).

Figure 13. US device assessing cortical bone thickness on point #4 of a marked right mandibular specimen.

3.3 Data Analysis

IBM SPSS Statistics 24.0 (IBM Corporation, Endicott, USA) was used to conduct the analysis. Paired t-test, Pearson correlation coefficient and the Bland Altman Plot were used to assess the agreement between cortical bone measurements obtained with μ-CT and US. Intra-rater reliability was assessed for μ-CT measurements by repeating the assessment on a scan of a specimen at a second time point and using an intra-class correlation coefficient test. The P-value was significant if ≤ 0.05.

Chapter 4: Results

4.1 Bone Model

Imagery obtained from both µ-CT and US scanning of the bone model were qualitatively compared. Striking similarities were found when comparing the x-plane from µ-CT with the C-scan from US (Fig. 14) and when comparing the z-plane from µ-CT with the B-scan from US (Fig. 15). The pulp canal is clearly defined in the US C-scan and correlates well with that of the µ-CT image in the x-plane. The US B-scan was able to delineate the bone model surface and root contour which also correlate well with µ-CT imagery when examining the model in the z-plane.

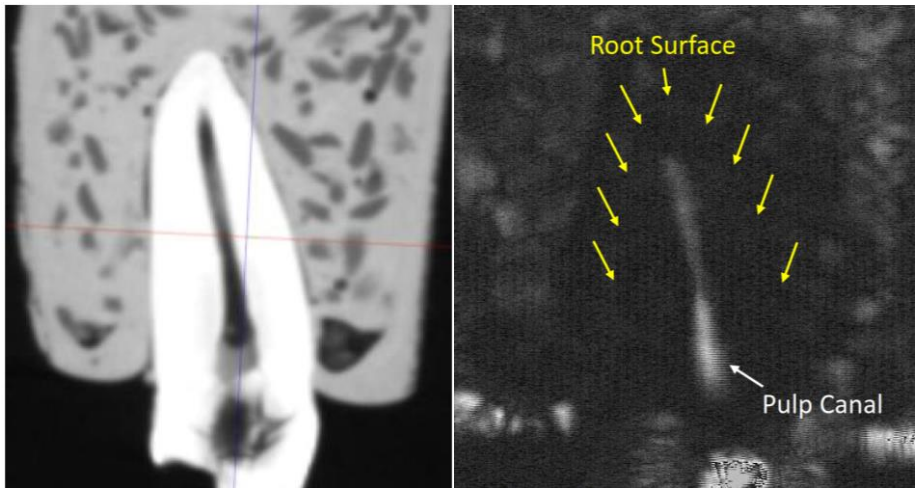

Figure 14. µ-CT scan x-plane slice (left) and US C-scan image (right) with pulp canal and root surface outline labeled.

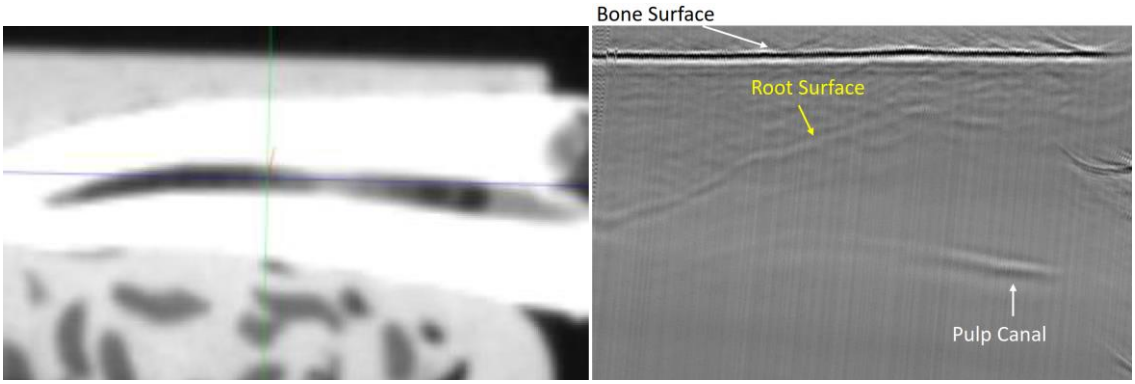

Figure 15. µ-CT scan z-plane slice (left) and US B-scan image (right). Interpretations of bone surface, root surface and pulp canal labeled on the US image.

A-scan imagery was also useful in the detection of the root as well as in the assessment of model cortical bone thickness over the embedded tooth root (Fig. 16). The formula for distance was used with the time between echoes from the bone surface and root obtained from A-scan imagery to determine model bone thickness. Thickness obtained from A-scan 1 is 1.31mm and A-scan 2 is 0.52mm.

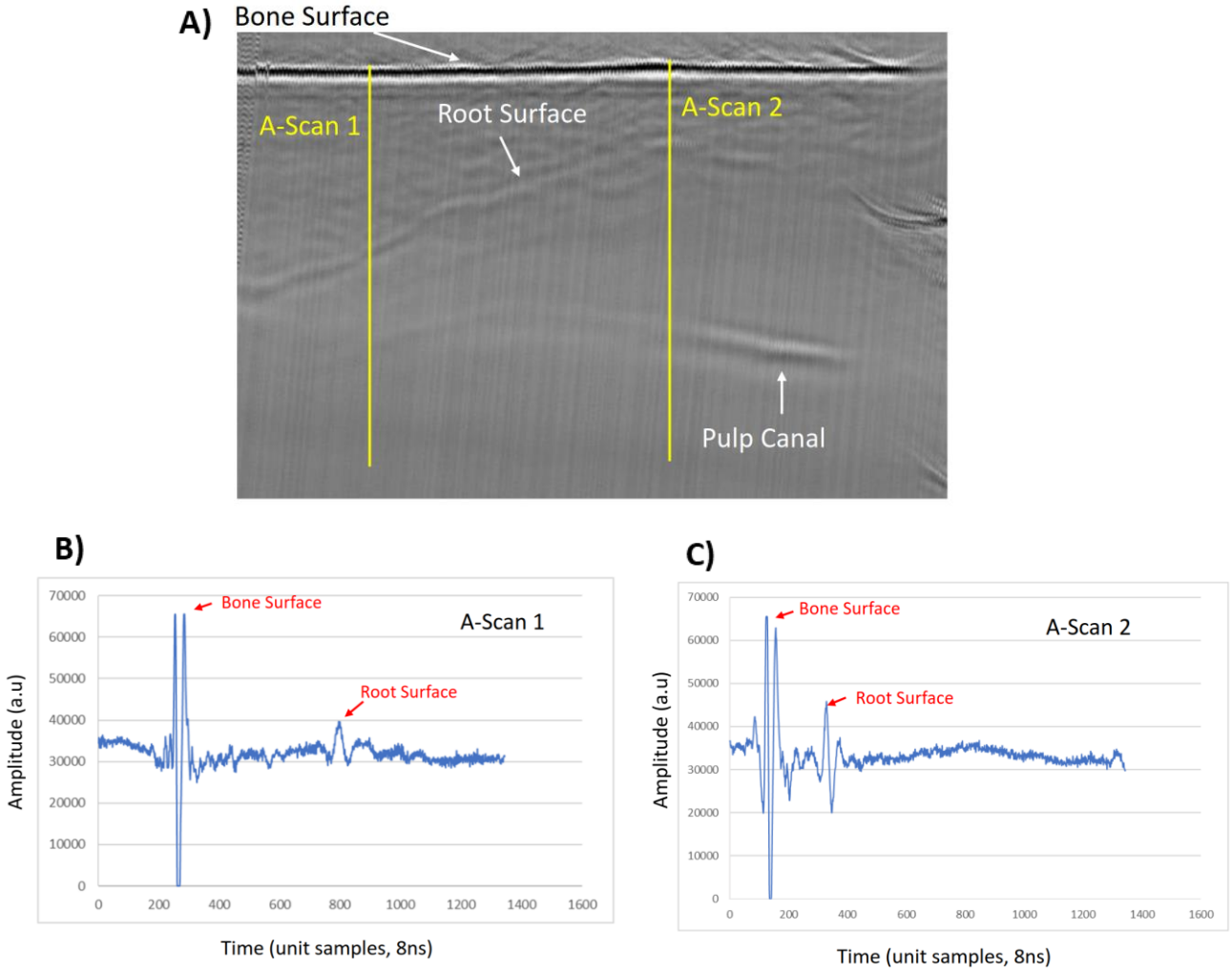

Figure 16. (A) US B-scan with points where A-Scan 1 and A-Scan 2 were taken from. **(B)** US A-Scan 1 image with bone surface and root surface peaks labelled corresponding to bone thickness of 1.31mm. **(C)** US A-Scan 2 image with bone surface and root surface peaks labelled corresponding to bone thickness of 0.52mm.

4.2 SOS Calibration: Porcine Specimen

The prepared bone sample was measured 10 times with a digital caliper for thickness and scanned with the US device 10 times to measure the TOF (Fig. 17). The mean thickness measurement was 1.01mm and the mean TOF for the sample was 0.62μS. These means were used with the previously mentioned formula to determine the SOS in our porcine cortical bone to be 3235m/s.

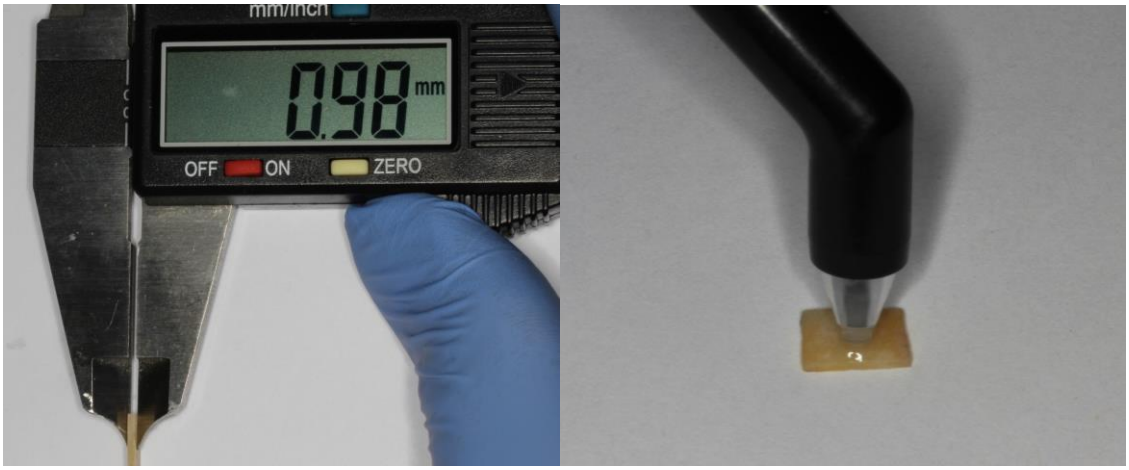

Figure 17. Cortical bone sample having thickness measured with digital calipers (left). TOF assessment with US device (right).

4.3 Comparison of μ-CT and US measurements

Cortical bone thickness measurements were first conducted from μ-CT scans of the specimens while at the same time recording the distance of the point away from the first or second premolar cusp tip line. 36 points were assessed from the 3 specimens. The mean cortical bone thickness (+/-SD) from μ-CT was 2.06+/-0.76mm with a range of 1.14-4.22mm. After labeling the appropriate landmarks and points on the specimens, US scans were conducted with the device. The software analyzed A-scans for three distinct peaks during scanning (Fig. 18). Once 20 successful scans were obtained, the algorithm averaged the TOFs and output a thickness measurement value based on our calibrated SOS. The mean cortical bone thickness from US was 1.61+/- 0.46mm with a range of 1.09-2.91mm.

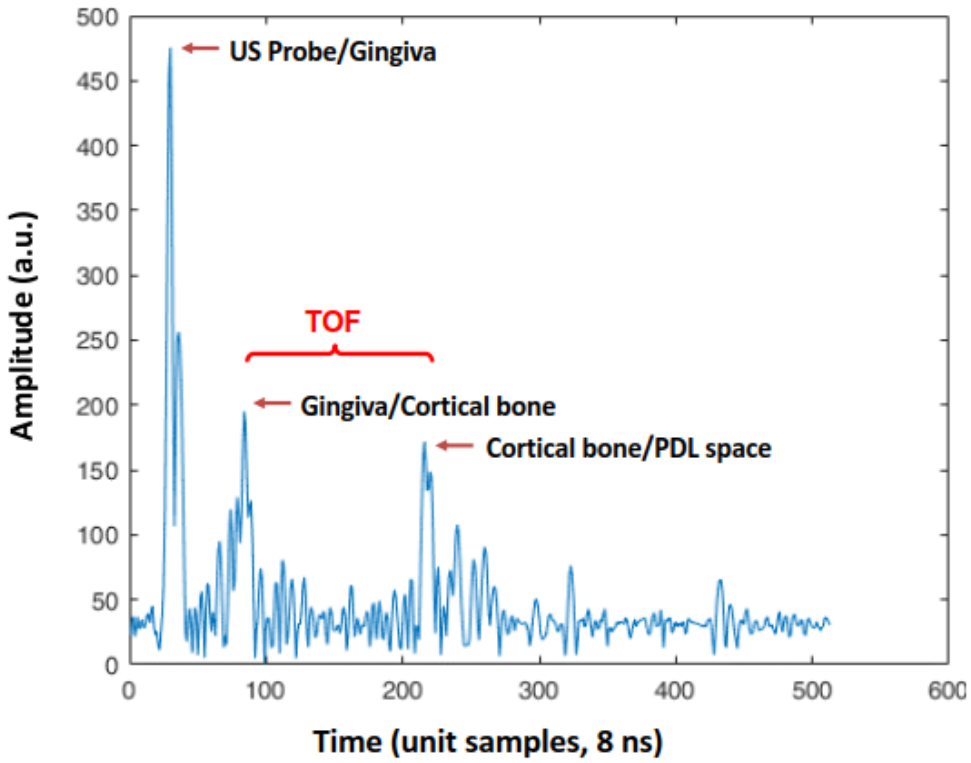

Figure 18. A-scan derived from US with peaks corresponding to echoes of waves from different tissue interfaces. Ideally, the first peak would correspond to probe/gingiva interface, second peak to gingiva/bone interface and third peak to bone/PDL interface. 8 nanoseconds per unit sample. Time of flight (TOF) is time difference between echoes from gingiva/bone and bone/PDL interfaces.

Table 1. Cortical bone thickness measurements obtained with μ -CT and US scans.

Method	n	Mean (mm)	SD
Micro-CT	36	2.06	0.76
Ultrasound	36	1.61	0.46

4.3.1 Analysis of Complete Data Set

Cortical bone measurements obtained by μ-CT and US were significantly different when analyzing the full data set (P=0.001). A scatterplot of the results shows a weak positive correlation with r= 0.369 (P=0.027) (Fig. 19).

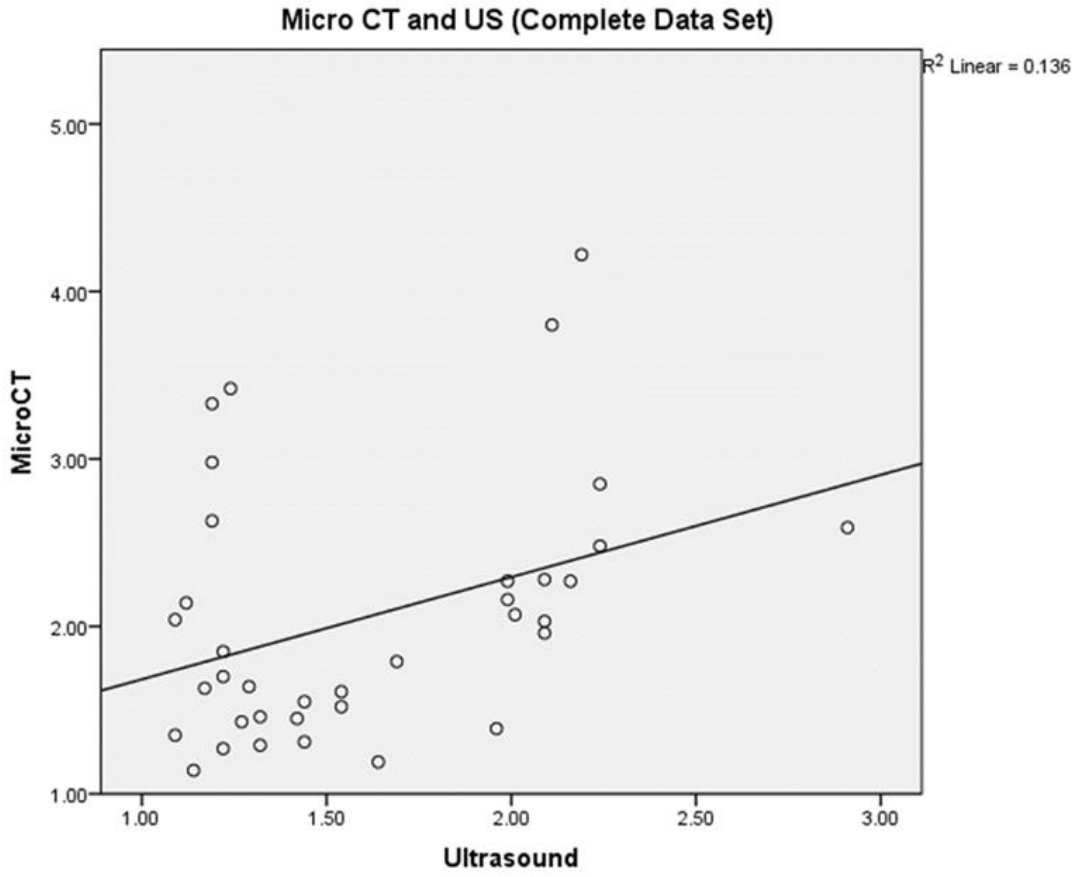

Figure 19. Scatterplot of the correlation between cortical bone thickness measurements obtained by µ-CT and US scanning in the complete data set (r=0.369).

A Bland-Altman plot was constructed to be able to further assess the agreement between the two methods. Each individual point of measurement is assessed for the difference between the two methods of measurement and plotted against the mean of the measurements for that same point (Fig. 20). The mean difference, or bias, was 0.45mm with a 95% confidence interval (CI) of 0.20-0.69mm. Because the line of equality, 0mm bias, did not fall within the 95% CI, the two methods of measurement can be said to not be in agreement.

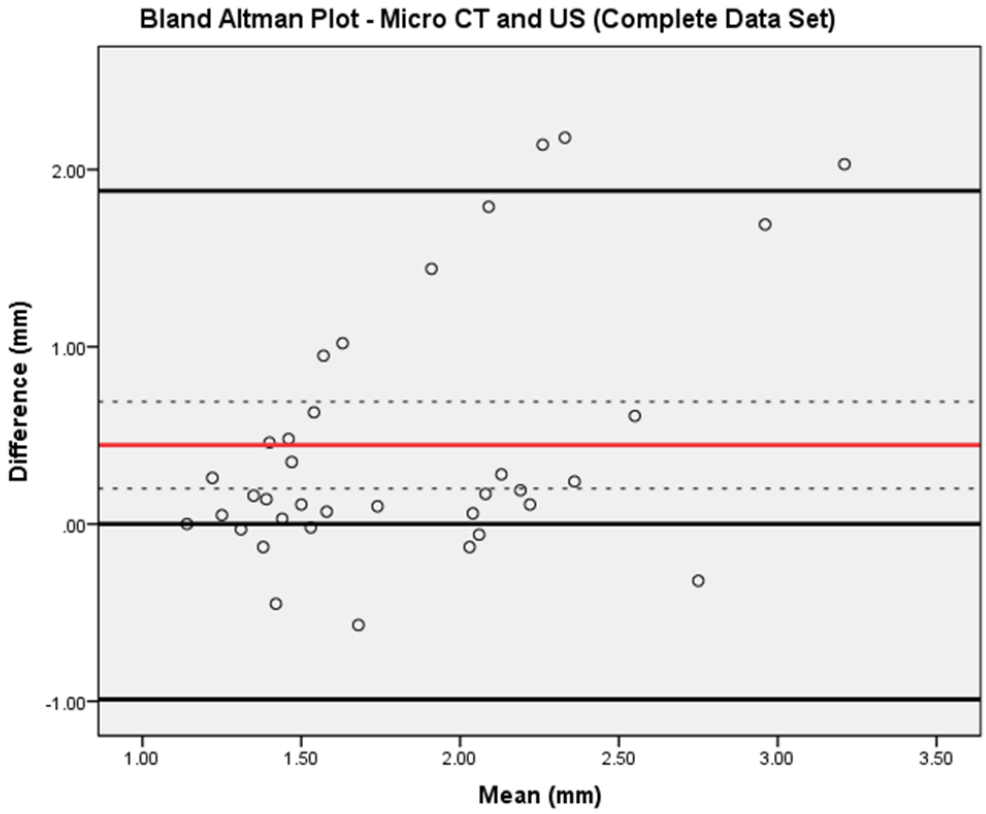

Figure 20. Bland Altman Plot with bias of 0.45mm (red line) and 95% CI of the bias (dotted lines). The line of equality, difference of 0mm, is outside the 95% CI of the bias.

4.3.2 Analysis Excluding µ-CT Points > 2.5mm Cortical Bone Thickness

Points in the data set with µ-CT cortical bone measurements of greater than 2.5mm were removed leaving a total of 28 points. The decision was made to exclude these points as human buccal cortical bone is rarely thicker than 2.5mm with the exception of the posterior mandible.[68] Mean cortical bone thickness from µ-CT was 1.72 +/- 0.39mm with a range of 1.14-2.48mm. The mean cortical bone thickness measurement from US was 1.56 +/- 0.39mm with a range of 1.09-2.24mm. Measurements obtained by µ-CT and US with the adjusted data set were significantly different (P=0.019). A scatterplot of the results shows a strong positive correlation with r= 0.613 (P=0.001) (Fig. 21).

Table 2. Cortical bone thickness measurements for adjusted data set (μ-CT <2.5mm).

Method	n	Mean (mm)	SD
Micro-CT	28	1.72	0.39
Ultrasound	28	1.56	0.39

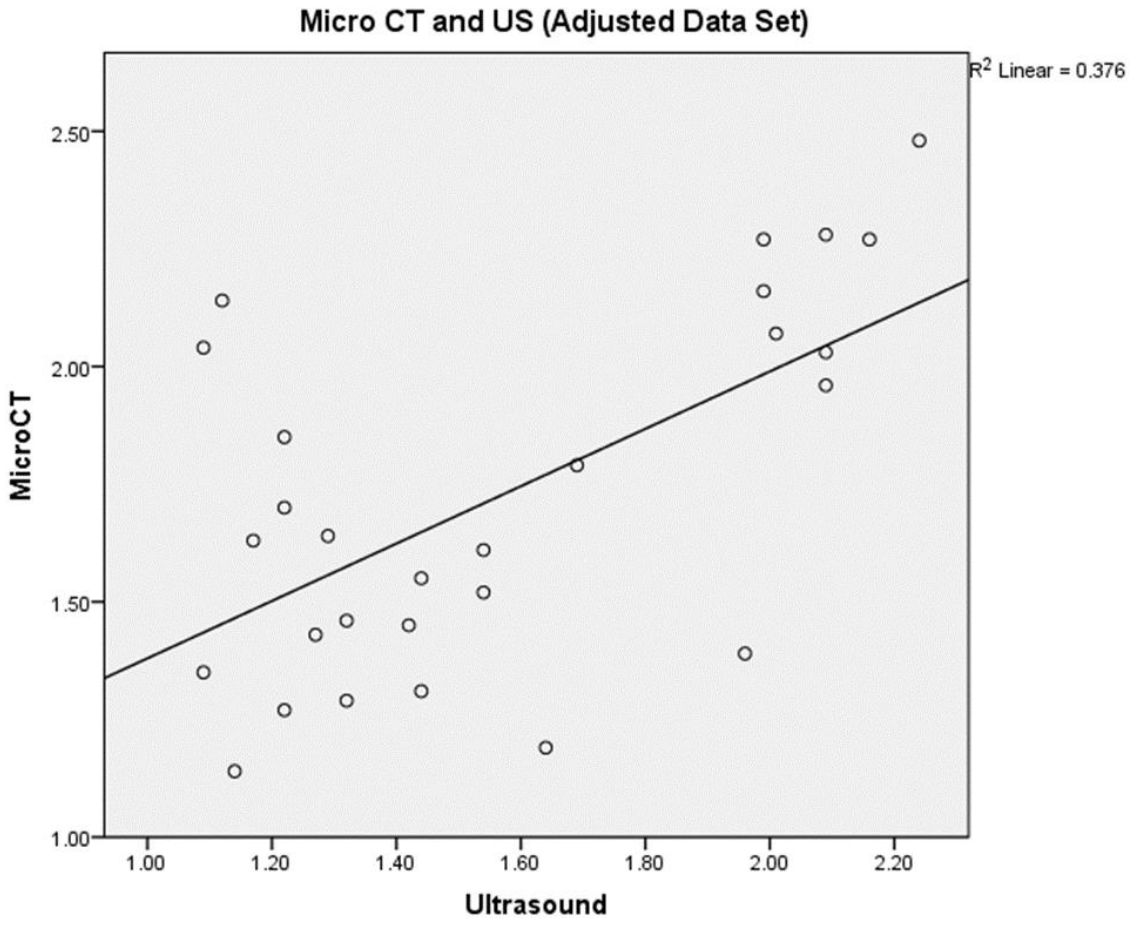

Figure 21. Scatterplot of the correlation between cortical bone thickness measurements obtained by μ-CT and US scanning without μ-CT >2.5mm (Adjusted Data Set) (r =0.613).

A new Bland-Altman plot was constructed from the adjusted data set (Fig. 22). The new bias was 0.16mm with a 95% CI of 0.03-0.29mm. The line of equality is much closer to the 95% CI of the bias but still falls outside of it. As such, the methods of measurement can still be said to not be in agreement.

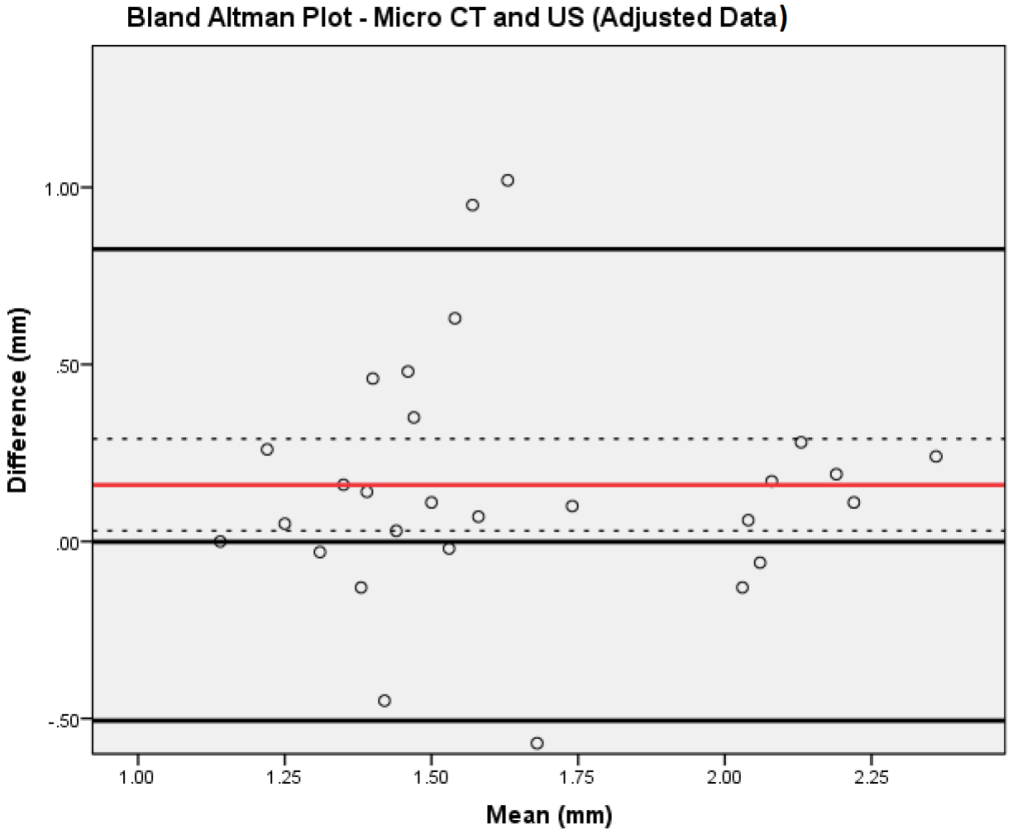

Figure 22. Bland Altman Plot without μ-CT >2.5mm (Adjusted Data Set) with bias of 0.16mm (red line) and 95% CI of the bias (dotted lines). The line of equality, difference of 0mm, is outside the 95% CI of the bias.

4.4 Intra-rater Reliability

An online digital number randomizer (True Random Number Service) was used to determine which of the 3 specimen would be selected for the intra-rater reliability assessment.[69] μ-CT bone thickness measurements were obtained a second time, 60 days after the original measurement. Intraclass correlation coefficient analysis showed an excellent correlation of 0.964 between the two sets of measurement ($P < 0.001$).

Chapter 5: Discussion

Periodontal complications such as gingival recession, bony dehiscence, and fenestration, are considerable adverse effects of orthodontic treatment when the orthodontist fails to recognize patients who might be susceptible to these issues. Initially thin cortical bone as well as excessive expansion and proclination or retraction out of the bony alveolar housing are significant risk factors for these problems. Dental CBCT can potentially be used to evaluate the periodontal hard tissues prior to treatment but the radiation exposure to the patient dictates that it should be used in limited situations. There exists a need for a non-radiative, cost-effective, and reliable method to assess cortical bone thickness prior to starting orthodontic treatment. The purpose of this investigation was to validate the use of a novel US device in the measurement of cortical bone thickness over roots in porcine mandibular specimens.

5.1 Jaw and Cortical Bone Models

Both jaw and cortical bone models were necessary for refinement of the US software, algorithms, and protocols. Upon US scanning of the larger jaw model, it became apparent that the cancellous bone layer that was placed between the tooth roots and the cortical bone layer made detection of the roots very difficult and unpredictable. The multi-locular, spongy structure of this layer possibly scattered both incident waves and echoes to the point that they could no longer be detected in A-scan or B-scan images. Focused transducers performed better than non-focused transducers because of the higher concentration of US energy in the areas of investigation. The decision was made to make a smaller cortical bone model embedded with a single tooth and US scan it with a focused 25MHz transducer in

the acoustic microscope to further refine the algorithms and software. This model was μ-CT scanned for qualitative comparison with our US scans.

Images from the US and μ-CT scans were analyzed and showed promising similarities when qualitatively assessing model bone thickness and root contour. The pulp canal of the tooth was clearly visible in both US B-scan and C-scan images. This is because of the drastic contrast and difference in impedance between the canal and the surrounding dentin/root. The canal was open to the environment and filled with air which has a much lower impedance (400 Rayl)[70] than that of dentin (7.8 MRayl)[71]. Impedance between root structure and overlying model bone (6.3MRayl)[66] are more similar, hence, the subtler delineation in US images. The tooth was directly embedded into the model material and did not have a mock PDL space. Incorporating a PDL space would have possibly made the junction between the tooth and model bone more visible on US scans. The proof of concept model bone experiments allowed our collaborators to improve and refine the software and algorithms to be used for the porcine specimen experiment.

5.2 SOS in Cortical Bone

The SOS through cortical bone has been reported as being highly variable. It is dependent on the elastic properties of the bone which readily change, especially in aging, as bone is a dynamic structure.[11,72,73] Different regions of human cortical bone have shown different SOS values. Cranial cortical bone has SOS values ranging from 2500-2960 m/s while femoral and tibial bone have shown a SOS from 3565-3800 m/s.[6,11,74]

Cortical bone in animal models also shows great variability. Porcine cortical bone mean SOS values from a study by Rose *et al.*[75] range from 2186– 3951m/s depending on the direction of wave propagation and physical maturity of the specimen. The vast range of reported values as well as the uncertainty of the exact age of our specimens due to pigs being slaughtered based on weight rather than age, drove us to calibrate the speed of sound for cortical bone in our porcine mandibles.

Our value of 3235m/s is within the range of SOS values reported in previous literature. Temperature is another factor that can potentially impact SOS through bone.[76] Our specimens were all stored at 0 degrees Celsius but were slowly brought to room temperature before conducting US measurements.

5.3 Agreement between Methods

Mean cortical bone thickness measurement with US was lower than that obtained with μ-CT. This is similar to results found by Nguyen *et al.*[25] in their study using a 20MHz US transducer on anterior porcine specimens. A possible explanation is the presence of vascular channels in cortical bone (Fig. 23). The software was designed to detect three distinct peaks and base the distance echoes travelled calculation on the time of flight between the second and third peak. This theoretically corresponds to the distance travelled between the gingiva/cortical bone interface and the cortical bone/PDL interface giving the thickness of cortical bone. During μ-CT analysis, vascular channels were sometimes present in proximity to points where thickness measurements were done. These vascular channels could

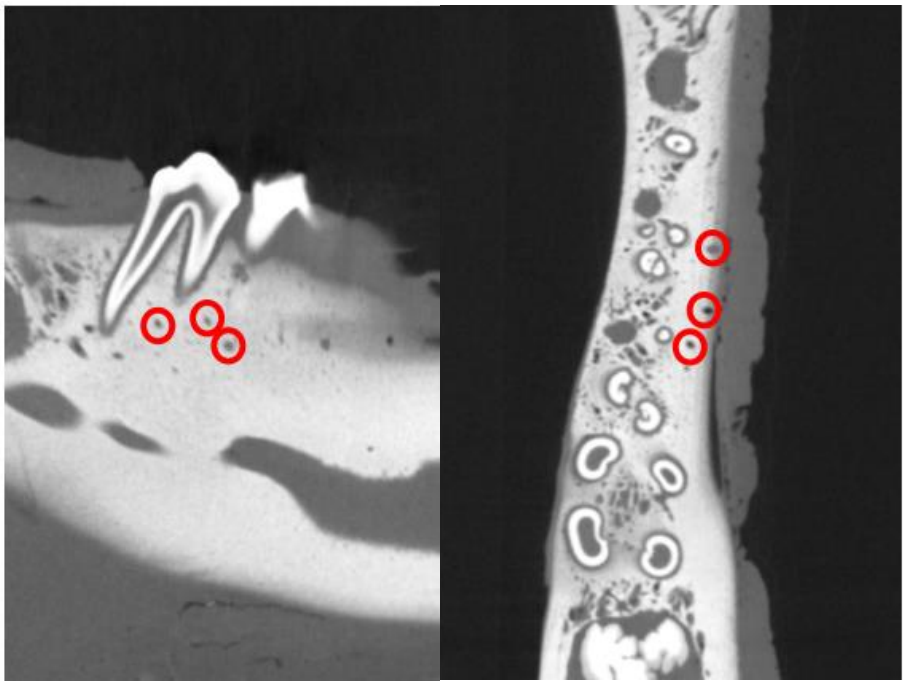

Figure 23. μ-CT scans of a specimen with several vascular channels outline (red circles) between the roots and the buccal cortical bone surface.

be responsible for producing a peak in the A-scan which would falsely be identified as the PDL/root and hence underestimating the thickness of cortical bone. This would not be expected to be an issue in humans, especially in younger and fully dentate subjects (the majority of orthodontic patients)who would have lower alveolar cortical bone porosity.[77]

The variability and discord between the two methods of measurement was greater if the μ-CT measurement was more than 2.5mm. Alveolar cortical bone thickness greater than this is rarely found in humans with the exception of the posterior mandible.[68] The increased variability in thicker bone may be explained by the larger distance that echoes would have to travel decreasing the probability of useful echoes from a conical root/PDL being detected by the transducer. For example, if echoes reflecting from a conical root only travel 1.5mm back to the transducer, a greater proportion of them will be detected as opposed to echoes from the same conical root having to travel 3.0mm back to the transducer.

The variability with thicker bone can also be explained by penetrance of the frequency of transducer used. The intra-oral device used a single focused transducer with a frequency of 19MHz. Lost *et al.*[16] showed a consistent penetrance of up to 1.5mm with a 20MHz on *in-vitro* bone sample models while a 5 MHz transducer penetrated up to 2mm consistently. The tradeoff with the lower frequency transducer was resolution and accuracy. The 19MHz transducer may have been too high frequency to reliably penetrate the bone and detect roots or PDL space in some of the thicker areas measured. Comparison of the data removing points with μ-CT measurements greater than 2.5mm, supports both of these explanations.

Although a variety of statistical tests were used to assess the agreement between the two measures, it can be argued that results from the Bland Altman plot are most appropriate. This statistical test assesses the average of the differences between paired methods of measurement which is more representative of agreement than how the measurements themselves are correlated.[78] One test can be

highly correlated to a gold standard but can still be inaccurate if it is off by the same amount each time. This is why the Bland Altman plot is the most popular statistical method to assess agreement between two medical instruments measuring continuous variables.[79]

5.4 μ-CT Measurements

Measurement of cortical bone thickness by means of μ-CT was used as the reference method for comparison. It is an extremely accurate, non-destructive method for bone structure assessment and has thus largely eclipsed histomorphometry and direct histological assessment as the gold standard method of analysis in the field.[63–65] The reorientation of the planes allowed for a thickness measurement that was perpendicular to the surface of the bone while simultaneously ensuring the measurement was done at the thinnest part over the root. The intra-rater reliability assessment showed that μ-CT measurements were highly repeatable (ICC=0.964) further showing the validity of using it as a reference.

5.5 US Device and Measurements

The novel US device was practical and straightforward to use for bone thickness measurements on the porcine samples. Although it wasn't used intra-orally, its compact size and ease of use lends itself to intra-oral use in the dental and orthodontic setting. The gathering of US data while scanning proved to be somewhat technique sensitive as the probe tip needed to be steadily held over the desired point until the software processed the required 20 successful A-scans to give a bone thickness measurement. The orientation of the probe tip was generally held flat against the surface of specimen allowing for perpendicular transmission of the US waves. Slight corrections to the orientation were sometimes needed to allow for successful A-scan readings.

Diagnostic US is dependent on the angulation and geometry of wave propagation and tissue boundaries. Detection of echoes from tissue boundaries and objects, what makes diagnostic US useful, is complicated by oblique incidence of US waves causing reflection away from the transducer and refraction of propagating waves as previously discussed (Fig.2 and Fig.3). One of the challenges of measuring cortical bone thickness with US is that the surfaces of the cortical bone and root/PDL space are rarely perfectly parallel especially apically (Fig. 24), as was also noted by Lost *et al.*[17] This results in only a portion of the useful echoes being detected by the transducer if at all in very divergent root/bone surface situations. This geometric dependence is not only seen in the buccal-lingual direction, it is also noted in the mesio-distal direction. Roots and PDLs are conical structures that have the potential to reflect US echoes away from the transducer.

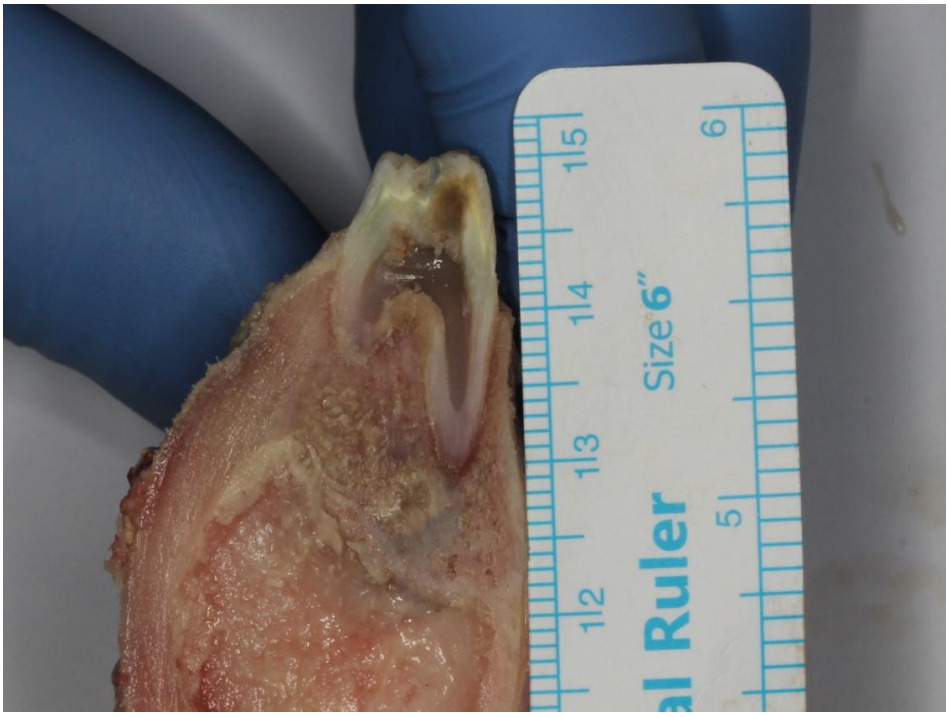

Figure 24. Cross-section of porcine tooth and mandible with the buccal surface to the right. The divergence of root/PDL and the surface of the cortical bone becomes more prominent further apically.

Although there was a protocol in place for extrapolating the points where measurements were done on the μ-CT and transferring them to the specimen for US assessment, this proved to be somewhat technically challenging. The mobility of the soft tissues made it difficult to precisely mark them with the surgical marker. Radiopaque metal markers could have possibly been placed in the samples prior to μ-CT but they would have had to have been placed a certain distance away from the points of interest because of their potential beam hardening effects. This would also not make it any less difficult to extrapolate and precisely locate points to be marked on the specimens. Once marked, the 1.5mm probe tip diameter of the US device was slightly larger than desirable to ensure accurate placement over the identified point for US measurement. A 1.0mm probe tip could have potentially ensured more accurate placement of the device.

5.6 Strengths of the Study

There were various strengths of our experiment. Firstly, the use of the larger jaw bone model and smaller cortical bone model allowed our collaborators to improve and refine software algorithms. It also allowed us to select the US method (pulse-echo) and type of transducer (single-focused) that would allow for best results in our porcine experiments.

The US device that was used to assess the porcine mandibles was specifically designed for intra-oral use. It is lightweight, compact, and easy to use/tolerate in the oral cavity. This is in contrast to studies that focused on table-top *in-vitro* experiments with fixed transducers in water baths[16–18,26], or those that used US devices designed for dermal use[24,25].

We used porcine specimens for our study which has proven to be an ideal model because of similarities to human jaw anatomy and function.[80] Although the cortical bone in certain parts of the porcine jaw is thicker and more vascular, and

the dental anatomy differs from humans, the porcine model does replicate how US waves would behave in human jaws with similar periodontal structures.

The SOS was calibrated for our porcine cortical bone samples. Because of the varying reports of SOS values in porcine bone in the literature, and the effect that age and maturity can have, measurement of SOS was conducted. This allowed us to calibrate our software and allow for more accurate bone thickness measurements with the US device.

Lastly, intra-rater reliability was assessed for μ-CT measurements by measuring cortical bone thickness for a specimen, 2 months after it was originally measured. Good repeatability and consistency were seen with measurements done from the gold standard μ-CT scans. Although intra-rater reliability was not possible to do for US measurements because of the time sensitive nature of the specimens, the software compensated by using mean TOF from 20 A-scans for thickness determination.

5.7 Limitations of the Study

The study has some limitations with the most notable one being the frequency of transducer used. As previously mentioned, the 19MHz transducer used may not have the bone penetrance to be able to detect and reflect echoes from roots in thicker areas of bone. The device could potentially be modified to use a 5MHz or 10MHz single focused transducer which would increase the depth of penetrance while likely still maintaining the resolution required for accurate bone thickness measurements.

The protocol for transferring points measured on μ-CT onto the specimens for US measurement was logical and straightforward. The act of labelling the points directly on the specimen was more difficult than originally thought which can be seen as a limitation due to possible inaccuracy. The size of the tip diameter on the US device, 1.5mm, could possibly contribute to inaccuracy of placement and a smaller tip diameter could increase placement accuracy.

The sample size of n=36 is adequate, but the fact that the points came from three hemi-mandibles from two pigs, could be seen as a limitation. This study should be viewed as a pilot study for future research to be conducted with a larger and possibly more varied sample size with the caveat that small SOS deviations could be expected amongst cortical bone from different pigs based on age and maturity. The variation in SOS values could also be a limitation in US measurement of cortical bone in human subjects as orthodontic patients vary greatly in maturity and bone mineral density. This issue could potentially be resolved by the establishment of normative SOS values for variables such as gender and age.

5.8 Clinical Relevance

Because of the periodontal complications that can arise during orthodontic treatment in patients with risk factors such as thin buccal cortical bone, a reliable and practical method to assess cortical bone thickness prior to starting orthodontic treatment is warranted.

Cortical bone measurements would be greatly beneficial in diagnosing and treatment planning an orthodontic case. Thin cortical bone measurements would warn the orthodontist about the risk of negative periodontal sequelae like gingival recession and bone dehiscence. This would potentially improve treatment planning, especially in moderately to severely crowded cases in which both expansion/proclination to increase arch length or extraction of permanent teeth are feasible treatment options. Thin cortical bone in these cases would indicate that extraction of permanent teeth would potentially allow the rest of the dentition to remain well within the bony alveolar housing as opposed to non-extraction treatment.

The only current method of assessing cortical bone thickness in the orthodontic setting is by using dental CBCT. As previously discussed, the accuracy of assessing and measuring bone thickness with CBCT is still not completely known,

especially in areas with cortical bone less than 1mm thick. The additional exposure to radiation with CBCT is also a concern which makes its only indications for routine use in orthodontics potentially very specific, such as in impacted teeth and skeletal asymmetries.

US has the potential to be useful in this regard as it is non-invasive, safe, and easy to use. With further improvements to the device used in this study, accurate and rapid cortical bone measurements appear to be possible.

5.9 Suggestions for Future Research

Pulse-echo US with a handheld device shows promise in measuring cortical bone thickness. Modifications to the device used in our study, such as a lower frequency transducer and a smaller diameter tip, as well as improvements and refinements in software and algorithms may allow it to be a clinically useful diagnostic tool.

Future research should be dedicated to experimenting with different frequency transducers and software/algorithm modifications to further compare US to the gold standard μ-CT. CBCT, used in the orthodontic setting, should also be used as a method for comparison with US.

Because of the difficulties encountered with porcine jaw and tooth anatomy and the non-invasive nature of US, human studies could also be conducted with essentially no risk. Orthodontic patients scheduled to undergo a CBCT for other diagnosis and treatment planning purposes (i.e. permanent tooth impactions or other pathology) could be recruited to be part of the study in the measurement of buccal cortical bone. Measurements obtained with the US device close to the CBCT scan date could then be compared to those obtained from CBCT imagery in these patients.

Chapter 6: Conclusion

A novel handheld ultrasound device showed promise in measuring cortical bone thickness over the roots of teeth in porcine mandibular specimens, but some degree of variability existed, especially when measuring thicker areas of bone. Further improvements to the device and algorithms used are warranted to increase the accuracy and reliability of this diagnostic tool.

References

1. Kremkau, F. W. & Forsberg, F. *Sonography: principles and instruments*. (Elsevier/Saunders, 2011).

2. Eklof, B., Lindström, K. & Persson, S. *Ultrasound in clinical diagnosis: from pioneering developments in Lund to global application in medicine*. (Oxford University Press, 2012).

3. Dalecki, D., Mercado, K.P., Hocking, D.C. Quantitative Ultrasound for Nondestructive Characterization of Engineered Tissues and Biomaterials. *Ann. Biomed. Eng.* **44**, 636-648 (2016).

4. Elahi, M. M., Lessard, M. L., Hakim, S., Watkin, K. & Sampalis, J. Ultrasound in the assessment of cranial bone thickness. *J. Craniofac. Surg.* **8**, 213–221 (1997).

5. Elahi, M. M., Watkin, K. L., Hakim, M. S., Schloss, M. D. & Lessard, M. L. A new predictive modality of cranial bone thickness. *Ann. Plast. Surg.* **42**, 651–657 (1999).

6. Tretbar, S. H., Plinkert, P. K. & Federspil, P. A. Accuracy of Ultrasound Measurements for Skull Bone Thickness Using Coded Signals. *IEEE Trans. Biomed. Eng.* **56**, 733–740 (2009).

7. Mujagic, M., Ginsberg, H. J. & Cobbold, R. S. C. Development of a method for ultrasound-guided placement of pedicle screws. *IEEE Trans. Ultrason. Ferroelectr. Freq. Control* **55**, 1267–1276 (2008).

8. Aly, A.-H., Ginsberg, H. J. & Cobbold, R. S. C. On Ultrasound Imaging for Guided Screw Insertion in Spinal Fusion Surgery. *Ultrasound Med. Biol.* **37**, 651–664 (2011).

9. Yamada, M., Moriya, H., Lino, T., Kasai, Y., Sudo, A. Uchida, A. Ultrasonic measurement of bone thickness for spinal surgery. *IEEE Trans. Ultrason. Ferroelectr. Freq. Control* **59**, 2077–2088 (2012).

10. Miller, P. D. Underdiagnoses and Undertreatment of Osteoporosis: The Battle to Be Won. *J. Clin. Endocrinol. Metab.* **101**, 852–859 (2016).

11. Karjalainen, J., Riekkinen, O., Töyräs, J., Kröger, H. & Jurvelin, J. Ultrasonic assessment of cortical bone thickness in vitro and in vivo. *IEEE Trans. Ultrason. Ferroelectr. Freq. Control* **55**, 2191–2197 (2008).

12. Karjalainen, J. P., Riekkinen, O., Töyräs, J., Jurvelin, J. S. & Kröger, H. New method for point-of-care osteoporosis screening and diagnostics. *Osteoporos. Int.* **27**, 971–977 (2016).

13. Jamal, S. A., Gilbert, J., Gordon, C. & Bauer, D. C. Cortical PQCT Measures Are Associated With Fractures in Dialysis Patients. *J. Bone Miner. Res.* **21**, 543–548 (2006).

14. Karjalainen, J. P., Riekkinen, O., Töyräs, J., Hakulinen, M., Kröger, H., Rikkonen, T., Salovaara, K., Jurvelin, J. S. Multi-site bone ultrasound measurements in elderly women with and without previous hip fractures. *Osteoporos. Int.* **23**, 1287–1295 (2012).

15. Karjalainen, J. P., Riekkinen, O. & Kröger, H. Pulse-echo ultrasound method for detection of post-menopausal women with osteoporotic BMD. *Osteoporos. Int.* **29**, 1193–1199 (2018).

16. Löst, C., Irion, K. M. & Nüssle, W. Periodontal ultrasonic diagnosis: experiments on thin bony platelets and on a simulated periodontal ligament space. *J. Periodontal Res.* **23**, 347–351 (1988).

17. Löst, C., Irion, K. M. & Nüssle, W. Determination of the facial/oral alveolar crest using RF-echograms. An in vitro study on the periodontium of pigs. *J. Clin. Periodontol.* **16**, 539–544 (1989).

18. Löst, C., Irion, K. M. & Nüssle, W. Ultrasonic B-scans of the facial/oral periodontium in pigs. *J. Clin. Periodontol.* **16**, 534–538 (1989).

19. Tsiolis, F. I., Needleman, I. G. & Griffiths, G. S. Periodontal ultrasonography. *J. Clin. Periodontol.* **30**, 849–854 (2003).

20. Eger, T. Ultrasonic determination of gingival thickness Subject variation and influence of tooth type and clinical features. *J. Clin. Periodontol.* **23**, 839–845 (1996).

21. Salmon, B. & Le Denmat, D. Intraoral ultrasonography: development of a specific high-frequency probe and clinical pilot study. *Clin. Oral Investig.* **16**, 643–649 (2012).

22. Zimbran, A., Dudea, S. & Dudea, D. Evaluation of Periodontal Tissues Using 40MHz Ultrasonography. Preliminary report. *Med. Ultrason.* **15**, 6–9 (2013).

23. Slak, B., Daabous, A., Bednarz, W., Strumban, E. & Maev, R. G. Assessment of gingival thickness using an ultrasonic dental system prototype: A comparison to traditional methods. *Ann. Anat. Anat. Anz. Off. Organ Anat. Ges.* **199**, 98–103 (2015).

24. Radu, C., Eugenia, B. M., Mihaela, H., Andrea, S. & Florin, B. A. Experimental model for measuring and characterisation of the dento-alveolar system using high frequencies ultrasound techniques. *Med. Ultrason.* **12**, 127–132 (2010).

25. Nguyen, K.-C. T., Le, L., Kaipatur, N. R., Zheng, R. Lou, E.H. Major, P. W. High-Resolution Ultrasonic Imaging of Dento-Periodontal Tissues Using a Multi-Element Phased Array System. *Ann. Biomed. Eng.* **44**, 2874–2886 (2016).

26. Degen, K., Habor, D., Radermacher, K., Heger, S., Kern, J-S., Wolfart, S., Marotti, J. Assessment of cortical bone thickness using ultrasound. *Clin. Oral Implants Res.* n/a-n/a (2016). doi:10.1111/clr.12829

27. Culjat, M. O., Choi, M., Singh, R. S., Grundfest, W. S., Brown, E. R., White, S.N. Ultrasound detection of submerged dental implants through soft tissue in a porcine model. *J. Prosthet. Dent.* **99**, 218–224 (2008).

28. Lekholm, U. & Zarb, G. Patient selection and preparation. in *Tissue-integrated prostheses: osseointegration in clinical dentistry* 199–209 (Quintessence, 1985).

29. Klein, M. O., Grötz, K. A., Manefeld, B., Kann, P. H. & Al-Nawas, B. Ultrasound Transmission Velocity for Noninvasive Evaluation of Jaw Bone Quality In Vivo Before Dental Implantation. *Ultrasound Med. Biol.* **34**, 1966–1971 (2008).

30. Kämmerer, P. W., Kumar, V. V. Brullmann, D., Gotz, H., Kann, P. H., Al-Nawas, B., Klein, M. O.. Evaluation of ultrasound transmission velocity and 3-dimensional radiology in different bone types for dental implantology: a comparative ex vivo study. *Oral Surg. Oral Med. Oral Pathol. Oral Radiol.* **116**, e77–e84 (2013).

31. Kumar, V. V., Sagheb, K., Klein, M.O., Al-Nawas, B., Kann, P.H., Kammerer, P. W.. Relation between bone quality values from ultrasound transmission velocity and implant stability parameters – an ex vivo study. *Clin. Oral Implants Res.* **23**, 975–980 (2012).

32. Machtei, E. E., Zigdon, H., Levin, L. & Peled, M. Novel ultrasonic device to measure the distance from the bottom of the osteotome to various anatomic landmarks. *J. Periodontol.* **81**, 1051–1055 (2010).

33. Zigdon-Giladi, H., Saminsky, M., Elimelech, R. & Machtei, E. E. Intraoperative Measurement of the Distance from the Bottom of Osteotomy to the Mandibular Canal Using a Novel Ultrasonic Device. *Clin. Implant Dent. Relat. Res.* **18**, 1034–1041 (2016).

34. Huang, J., Li, J. & Wang, H. The Principles and Procedures of Ultrasound-guided Anesthesia Techniques. *Cureus* **10**, e2980 (2018).

35. Hafeez, N. S., Sondekoppam, R. V., Ganapathy, S., Armstrong, J. E., Shimizu, M., Johnson, M., Merrifield, P., Galil, K. A. Ultrasound-Guided Greater Palatine Nerve Block: A Case Series of Anatomical Descriptions and Clinical Evaluations. *Anesth. Analg.* **119**, 726–730 (2014).

36. Linkow, L. I. Implanto-Orthodontics. *J Clin Orthod* **4**, 685–690 (1970).

37. Kim, H.-J., Kim, D.-H., Yun, H.-S., Park, H.-D. & Park, Y.-C. Soft-tissue and cortical-bone thickness at orthodontic implant sites. *Am. J. Orthod. Dentofacial Orthop.* **130**, 177–182 (2006).

38. Cha, B.-K., Lee, Y.-H., Lee, N.-K., Choi, D.-S. & Baek, S.-H. Soft tissue thickness for placement of an orthodontic miniscrew using an ultrasonic device. *Angle Orthod.* **78**, 403–408 (2008).

39. Garib, D. G., Yatabe, M. S., Ozawa, T. O. & Silva Filho, O. G. da. Alveolar bone morphology under the perspective of the computed tomography: Defining the biological limits of tooth movement. *Dent. Press J. Orthod.* **15**, 192–205 (2010).

40. Graber, L. W., Vanarsdall, R. L., Jr & Vig, K. W. L. *Orthodontics: current principles and techniques*. (Elsevier/Mosby, 2012).

41. Proffit, W. R. *Contemporary orthodontics*. (Elsevier/Mosby, 2013).

42. Greenbaum, K. R. & Zachrisson, B. U. The effect of palatal expansion therapy on the periodontal supporting tissues. *Am. J. Orthod.* **81**, 12–21 (1982).

43. Garib, D. G., Henriques, J. F. C., Janson, G., de Freitas, M. R. & Fernandes, A. Y. Periodontal effects of rapid maxillary expansion with tooth-tissue-borne and tooth-borne expanders: A computed tomography evaluation. *Am. J. Orthod. Dentofacial Orthop.* **129**, 749–758 (2006).

44. Rungcharassaeng, K., Caruso, J. M., Kan, J. Y. K., Kim, J. & Taylor, G. Factors affecting buccal bone changes of maxillary posterior teeth after rapid maxillary expansion. *Am. J. Orthod. Dentofacial Orthop.* **132**, 428.e1-428.e8 (2007).

45. Årtun, J. & Grobéty, D. Periodontal status of mandibular incisors after pronounced orthodontic advancement during adolescence: A follow-up evaluation. *Am. J. Orthod. Dentofacial Orthop.* **119**, 2–10 (2001).

46. Årtun, J. & Krogstad, O. Periodontal status of mandibular incisors following excessive proclination A study in adults with surgically treated mandibular prognathism. *Am. J. Orthod. Dentofacial Orthop.* **91**, 225–232 (1987).

47. Sarikaya, S., Haydar, B., Ciğer, S. & Ariyürek, M. Changes in alveolar bone thickness due to retraction of anterior teeth. *Am. J. Orthod. Dentofacial Orthop.* **122**, 15–26 (2002).

48. Engelking, G. & Zachrisson, B. U. Effects of incisor repositioning on monkey periodontium after expansion through the cortical plate. *Am. J. Orthod. Dentofacial Orthop.* **82**, 23–32 (1982).

49. Thilander, B., Nyman, S., Karring, T. & Magnusson, I. Bone regeneration in alveolar bone dehiscences related to orthodontic tooth movements. *Eur. J. Orthod.* **5**, 105–114 (1983).

50. Wennström, J. L., Lindeh, J., Sinclair, F., Thilander, B. Some periodontal tissue reactions to orthodontic tooth movement in monkeys. *J. Clin. Periodontol.* **14**, 121–129 (1987).

51. Jäger, F., Mah, J. K. & Bumann, A. Peridental bone changes after orthodontic tooth movement with fixed appliances: A cone-beam computed tomographic study. *Angle Orthod.* **87**, 672–680 (2017).

52. Misch, K. A., Yi, E. S. & Sarment, D. P. Accuracy of Cone Beam Computed Tomography for Periodontal Defect Measurements. *J. Periodontol.* **77**, 1261–1266 (2006).

53. Molen, A. D. Considerations in the use of cone-beam computed tomography for buccal bone measurements. *Am. J. Orthod. Dentofacial Orthop.* **137**, S130–S135 (2010).

54. Leung, C. C., Palomo, L., Griffith, R. & Hans, M. G. Accuracy and reliability of cone-beam computed tomography for measuring alveolar bone height and detecting bony dehiscences and fenestrations. *Am. J. Orthod. Dentofacial Orthop.* **137**, S109–S119 (2010).

55. Patcas, R., Müller, L., Ullrich, O. & Peltomäki, T. Accuracy of cone-beam computed tomography at different resolutions assessed on the bony covering of the mandibular anterior teeth. *Am. J. Orthod. Dentofacial Orthop.* **141**, 41–50 (2012).

56. Mandelaris, G. A., Neiva, R. & Chambrone, L. Cone-Beam Computed Tomography and Interdisciplinary Dentofacial Therapy: An American Academy of Periodontology Best Evidence Review Focusing on Risk Assessment of the Dentoalveolar Bone Changes Influenced by Tooth Movement. *J. Periodontol.* **88**, 960–977 (2017).

57. Kapila, S. D. & Nervina, J. M. CBCT in orthodontics: Assessment of treatment outcomes and indications for its use. *Dentomaxillofacial Radiol.* **44**, 20140282 (2015).

58. De Grauwe, A., Ayaz, I., Shujaat, S., Dimitrov, S., Gbadegbegnon, L., Vande Vannet, B., Jacobs, R.. CBCT in orthodontics: a systematic review on justification of CBCT in a paediatric population prior to orthodontic treatment. *Eur. J. Orthod.* (2018). doi:10.1093/ejo/cjy066

59. White, S. C. & Pharoah, M. J. *Oral radiology: principles and interpretation*. (Elsevier/Mosby, 2014).

60. Sadek, M. M., Sabet, N. E. & Hassan, I. T. Alveolar bone mapping in subjects with different vertical facial dimensions. *Eur. J. Orthod.* **37**, 194–201 (2014).

61. Garlock, D. T., Buschang, P. H., Araujo, E. A., Behrents, R. G. & Kim, K. B. Evaluation of marginal alveolar bone in the anterior mandible with pretreatment and posttreatment computed tomography in nonextraction patients. *Am. J. Orthod. Dentofacial Orthop.* **149**, 192–201 (2016).

62. Antoun, J. S., Mei, L., Gibbs, K. & Farella, M. Effect of orthodontic treatment on the periodontal tissues. *Periodontol. 2000* **74**, 140–157 (2017).

63. Burghardt, A. J., Link, T. M. & Majumdar, S. High-resolution Computed Tomography for Clinical Imaging of Bone Microarchitecture. *Clin. Orthop.* **469**, 2179–2193 (2011).

64. Suttapreyasri, S., Suapear, P. & Leepong, N. The Accuracy of Cone-Beam Computed Tomography for Evaluating Bone Density and Cortical Bone Thickness at the Implant Site: Micro-Computed Tomography and Histologic Analysis. *J. Craniofac. Surg.* **29**, 2026–2031 (2018).

65. Kubíková, T. Bartos, M., Juhas, S., Suchy, T., Sauerova, P., Hubalek-Kalbacova, M., Tonar, Z. Comparison of ground sections, paraffin sections and micro-CT imaging of bone from the epiphysis of the porcine femur for morphometric evaluation. *Ann. Anat.* **220**, 85–96 (2018).

66. Wydra, A. & Maev, R. G. A novel composite material specifically developed for ultrasound bone phantoms: cortical, trabecular and skull. *Phys. Med. Biol.* **58**, N303 (2013).

67. Tonge, C. H. & McCance, R. A. Normal development of the jaws and teeth in pigs, and the delay and malocclusion produced by calorie deficiencies. *J. Anat.* **115**, 1–22 (1973).

68. Fayed, M. M. S., Pazera, P. & Katsaros, C. Optimal sites for orthodontic mini-implant placement assessed by cone beam computed tomography. *Angle Orthod.* **80**, 939–951 (2010).

69. Haahr, Mads. (2018, October 22). Random.org: *True Random Number Service*. Retrieved from https://www.random.org

70. Alvarez-Arenas, T. E. G. Acoustic impedance matching of piezoelectric transducers to the air. *IEEE Trans. Ultrason. Ferroelectr. Freq. Control* **51**, 624–633 (2004).

71. Singh, R., Brown, E., White, S., Grundfest, W. & Culjat, M. Tissue mimicking materials for dental ultrasound. *J. Acoust. Soc. Am.* **123**, EL39-EL44 (2008).

72. Zioupos, P. & Currey, J. D. Changes in the Stiffness, Strength, and Toughness of Human Cortical Bone With Age. *Bone* **22**, 57–66 (1998).

73. Misch, C. E., Qu, Z. & Bidez, M. W. Mechanical properties of trabecular bone in the human mandible: Implications for dental implant treatment planning and surgical placement. *J. Oral Maxillofac. Surg.* **57**, 700–706 (1999).

74. Wear, K. A. Autocorrelation and cepstral methods for measurement of tibial cortical thickness. *IEEE Trans. Ultrason. Ferroelectr. Freq. Control* **50**, 655–660 (2003).

75. Rose, E. C., Hagenmüller, M., Jonas, I. E. & Rahn, B. A. Validation of speed of sound for the assessment of cortical bone maturity. *Eur. J. Orthod.* **27**, 190–195 (2005).

76. Souza, R. M., Costa-Felix, R. P. B. & Alvarenga, A. V. The influence of temperature on the speed of sound of cortical bone phantom: A metrological view. in *Journal of Physics: Conference Series* **975**, (2018).

77. Kingsmill, V. J., Gray, C. M., Moles, D. R. & Boyde, A. Cortical Vascular Canals in Human Mandible and Other Bones. *J. Dent. Res.* **86**, 368–372 (2007).

78. Giavarina, D. Understanding Bland Altman analysis. *Biochem. Medica* **25**, 141–151 (2015).

79. Zaki, R., Bulgiba, A., Ismail, R. & Ismail, N. A. Statistical methods used to test for agreement of medical instruments measuring continuous variables in method comparison studies: A systematic review. *PLoS ONE* **7**, e37908 (2012).

80. Wang, S., Liu, Y., Fang, D. & Shi, S. The miniature pig: a useful large animal model for dental and orofacial research. *Oral Dis.* **13**, 530–537 (2007).

Appendices

Appendix A: Porcine Speed of Sound Calibration Raw Data

time (uS)	thickness(mm)
0.705	0.99
0.585	1.06
0.54	0.98
0.6074	1
0.5775	1.02
0.52	0.99
0.66	1
0.6825	1.04
0.6625	0.99
0.6725	0.98

Appendix B: Buccal Cortical Bone Thickness Measurements Raw Data

Sample point	μ-CT measurement (mm)	US measurement (mm)	Difference (mm)	Mean (mm)
1R1	2.07	2.01	0.06	2.04
1R2	2.16	1.99	0.17	2.08
1R3	2.27	1.99	0.28	2.13
1R4	4.22	2.19	2.03	3.21
1R5	2.59	2.91	-0.32	2.75
1R6	2.03	2.09	-0.06	2.06
1R7	2.28	2.09	0.19	2.19
1R8	2.48	2.24	0.24	2.36
1R9	2.85	2.24	0.61	2.55
1R10	2.27	2.16	0.11	2.22
1R11	1.96	2.09	-0.13	2.03
1R12	3.80	2.11	1.69	2.96
2L1	1.31	1.44	-0.13	1.38
2L2	1.27	1.22	0.05	1.25
2L3	1.52	1.54	-0.02	1.53
2L4	1.79	1.69	0.10	1.74
2L5	1.39	1.96	-0.57	1.68
2L6	1.43	1.27	0.16	1.35
2L7	1.63	1.17	0.46	1.40
2L8	1.64	1.29	0.35	1.47
2L9	1.45	1.42	0.03	1.44
2L10	1.61	1.54	0.07	1.58
2L11	3.33	1.19	2.14	2.26
2L12	3.42	1.24	2.18	2.33
2R1	1.19	1.64	-0.45	1.42
2R2	1.14	1.14	0.00	1.14
2R3	1.35	1.09	0.26	1.22
2R4	2.14	1.12	1.02	1.63
2R5	1.29	1.32	-0.03	1.31
2R6	1.46	1.32	0.14	1.39
2R7	1.70	1.22	0.48	1.46
2R8	2.63	1.19	1.44	1.91
2R9	1.55	1.44	0.11	1.50
2R10	1.85	1.22	0.63	1.54
2R11	2.04	1.09	0.95	1.57
2R12	2.98	1.19	1.79	2.09

Appendix C: Intra-rater Reliability Raw Data

	Micro CT measurements (mm)	
Specimen 2R (for ICC)	**T1**	**T2**
2R1	1.19	1.14
2R2	1.14	1.11
2R3	1.35	1.47
2R4	2.14	2.05
2R5	1.29	1.16
2R6	1.46	1.49
2R7	1.70	1.79
2R8	2.63	2.64
2R9	1.55	1.51
2R10	1.85	1.71
2R11	2.04	1.97
2R12	2.98	2.86

Appendix D: License to Reproduce Journal Figure

SPRINGER NATURE LICENSE TERMS AND CONDITIONS

Feb 04, 2019

This Agreement between Dr. Diego Diaz ("You") and Springer Nature ("Springer Nature") consists of your license details and the terms and conditions provided by Springer Nature and Copyright Clearance Center.

License Number	4522010230117
License date	Feb 04, 2019
Licensed Content Publisher	Springer Nature
Licensed Content Publication	Annals of Biomedical Engineering
Licensed Content Title	Quantitative Ultrasound for Nondestructive Characterization of Engineered Tissues and Biomaterials
Licensed Content Author	Diane Dalecki, Karla P. Mercado, Denise C. Hocking
Licensed Content Date	Jan 1, 2015
Licensed Content Volume	44
Licensed Content Issue	3
Type of Use	Thesis/Dissertation
Requestor type	non-commercial (non-profit)
Format	print and electronic
Portion	figures/tables/illustrations
Number of figures/tables/illustrations	1
Will you be translating?	no
Circulation/distribution	<501
Author of this Springer Nature content	no
Title	Diagnostic Ultrasound in the Measurement of Cortical Bone Thickness in Porcine Mandibular Specimens
Institution name	Western University
Expected presentation date	Feb 2019
Portions	Figure 1
Requestor Location	Dr. Diego Diaz
Billing Type	
Billing Address	
Total	**0.00 CAD**
Terms and Conditions	

Springer Nature Terms and Conditions for RightsLink Permissions

Curriculum Vitae

Diego Diaz

Post-secondary Education and Degrees:

University of British Columbia
Vancouver, British Columbia, Canada
2002-2007 B.Sc. (Hons)

Western University
Schulich Medicine and Dentistry
London, Ontario, Canada
2009-2013 D.D.S.

Western University
Schulich Medicine and Dentistry
London, Ontario, Canada
2016-2019 M.Cl.D.

Honours and Awards:

Golden Key Honour Society, University of British Columbia
2007
Dean's Honour List, Western University
2009-2013
Class of 1975 Scholarship for Academic Achievement, Western University
2012
Dr. Igor Bolta Memorial Award in Restorative Dentistry, Western University
2013
American Association of Oral and Maxillofacial Surgeons Award, Western University
2013
John and Nancy Murray Prize, Western University
2018
Research Day Poster Presentation Merit Award – Senior Category, Western University
2018
Dr. Bryan Smith Award in Graduate Orthodontics Western University
2019